

A Survey of High-Level Modeling and Simulation Methods for Modern Machine Learning Workloads

Anonymous Author(s)

Under Review

Anonymous

Abstract

We survey 25 performance modeling tools from 53 papers (2016–2026) and evaluate ten—NeuSight, ASTRA-sim, VIDUR, Timeloop, nn-Meter with full experiments, plus MAESTRO, Paleo, Habitat, Accel-Sim with deployment testing—across 146 GPU configurations, collective benchmarks, LLM serving, energy validation, and reproducibility testing. Three findings emerge: (1) self-reported accuracy is unreliable—NeuSight claims 2.3% MAPE but we measure 5.87–27.10%, while nn-Meter produces no output due to dependency rot; (2) the five tools are complementary but disjoint, motivating a unified pipeline; (3) the kernel-to-model composition gap (2–9% kernel error growing to 10–28% model error) dominates total error, yet no tool addresses this layer.

Keywords

ML workload performance prediction, DNN accelerator modeling, GPU simulation, distributed training simulation, LLM inference serving, design space exploration, survey

1 Introduction

Domain-specific architectures [25, 34, 35] make performance prediction critical, yet no prior work examines *why* certain approaches succeed or how errors propagate; prior surveys cover ML techniques for modeling [78], specific hardware, or distributed training simulators [77]. We contribute: (1) a **28-scenario benchmark suite** where 50% of scenarios lack tool support; (2) **third-party evaluation** showing claimed error rates are overstated by 2–4×; (3) a **unified pipeline** identifying the composition gap; and (4) a **research agenda** for composition modeling and continuous validation.

2 Survey Methodology

From 287 candidates on ACM DL, IEEE Xplore, Semantic Scholar, and arXiv, 53 papers (2016–2026) plus 12 foundational works were classified by methodology, platform, and abstraction level [66], excluding proprietary tools, infrastructure [6, 71], compilers [45, 64, 80], and schedulers [33, 63].

3 Background

ML workloads expressed in frameworks such as PyTorch [60] and TensorFlow [1] are computation graphs where performance depends on dataflow/tiling, KV cache [44], and compute–memory–network balance; LLM inference splits into compute-bound prefill and memory-bound decode [2, 61, 88], forcing serving systems to disaggregate or chunk requests [94]; at-scale challenges such as

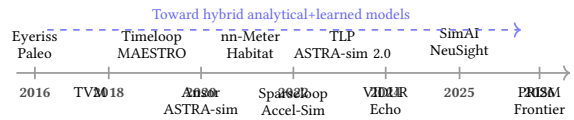


Figure 1: Evolution of performance modeling tools (2016–2026).

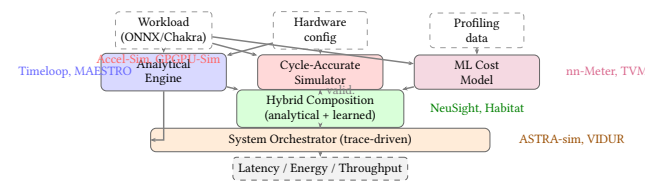


Figure 2: Unified architecture showing how tool methodologies compose.

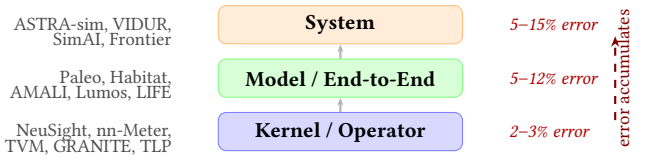


Figure 3: Abstraction level hierarchy with error accumulation.

expert parallelism [15] further complicate prediction. Five modeling types span accuracy–speed trade-offs: **analytical** [32, 85] (μ s), **cycle-accurate** [4, 30, 38] with memory models such as DRAM-Sim3 [50] and Ramulator [41, 53] (10^3 – 10^4 × slowdown), **trace-driven** [3, 86] (min.), **ML-augmented** [91] (ms), and **hybrid** [48, 89].

4 Taxonomy

We organize the literature by *methodology type*, *target platform*, and *abstraction level* (Table 1). Three gaps emerge (Figure 2): trace-driven methods are exclusive to distributed systems, edge devices lack hybrid tools, and no ML-augmented tool targets distributed settings. **Methodology–platform pairings.** Platform constrains methodology: accelerators use analytical models [43, 58]; GPUs span all five types; distributed systems need trace-driven simulation [3, 86]; edge relies on ML-augmented [18, 91]; CPUs remain the least studied platform [56]. Errors propagate (Figure 3): kernel 2–3%, model 5–12%, system 5–15%. **Workload coverage.** Of 14 tools, 9 validate only on CNNs; post-2023 tools target transformers/LLMs but **none validates on diffusion or dynamic inference**.

Table 1: Methodology taxonomy: coverage matrix and trade-off profile. 0 = research gap.

Methodology	DNN Accel.	GPU	Distrib. Systems	Edge/ Mobile	CPU	Eval. Speed	Data Req.	Interp.	Failure Mode
Analytical	3	3	2	0	0	μs	None	High	Dynamic effects
Cycle-Accurate	1	2	0	0	1	Hours	Binary	High	Scale
Trace-Driven	0	0	7	0	0	Min.	Traces	Med.	Trace fidelity
ML-Augmented	0	3	0	3	1	ms	Profiling	Low	Distrib. shift
Hybrid	1	2	0	0	1	ms	Mixed	Med.	Training domain

such as speculative decoding [9, 40]; only Frontier [20] covers MoE, whose expert-parallel routing introduces load-dependent latency that static models cannot capture.

5 Survey of Approaches

We survey tools by target platform (Table 2). **DNN accelerators and GPUs.** Analytical tools—Timeloop [58], MAESTRO [43], Sparseloop [87], SCALE-Sim [72], DianNao [11], PIM tools [26, 31, 46, 59], Arch-Gym [42]—enumerate mappings; cycle-accurate simulators [4, 38], validated with hardware counters [7, 81] and profilers [57], achieve 0.90–0.97 IPC correlation at 10^3 – 10^4 × slowdown; hybrid tools [5, 10, 12, 19, 23, 48, 82, 84, 89, 90, 92, 93] trade accuracy for speed; lightweight analytical alternatives such as Path Forward [51] use linear regression to achieve 7% error without simulation overhead. **Distributed/serving:** ASTRA-sim [86], SimAI [83], VIDUR [3], Lumos [52], PRISM [21], and others [8, 20, 24, 28, 36, 62, 73, 76, 94] cover training and serving, with parallelism strategies from Megatron-LM [74], GPipe [29], and ZeRO [65]; network effects are captured by detailed simulators such as NS-3 [70]; LitePred [18] and HELP [47] cover mobile [17, 55]. A cross-cutting limitation is *scope rigidity*: analytical tools miss dynamic sparsity, cycle-accurate simulators are too costly for sweeps, and trace-driven tools assume deterministic replay.

6 Evaluation Methodology

Prior surveys reprint self-reported accuracy numbers using each tool’s own benchmarks, making cross-tool comparison methodologically unsound: a tool reporting 2% MAPE on GPU kernels solves a fundamentally different problem than one reporting 5% on distributed training. We introduce a **third-party evaluation focusing on accuracy and feature coverage** that addresses this gap through two components. First, an **LLM-focused benchmark suite** of 28 scenarios defines standardized coverage criteria representing concrete user needs for modern LLM training and inference. Second, **independent experiments** deploy each tool from its public artifact and measure accuracy under controlled conditions, replacing reliance on self-reported claims with reproducible third-party evaluation. This framework is the first to systematically evaluate ML performance modeling tools through third-party testing rather than reprinting authors’ own results.

Evaluation principle. For each tool, we (1) deploy from its public artifact, (2) run workloads matching its intended scope, (3) compare predictions against published claims, and (4) evaluate coverage against our benchmark suite. Where absolute verification requires hardware we lack (e.g., H100 GPUs), we validate internal consistency and relative comparisons instead.

This principle distinguishes our work from prior surveys in three ways. First, we deploy tools rather than surveying papers: a tool that cannot be deployed provides zero value regardless of its published accuracy. Second, we measure accuracy independently rather than reprinting self-reported numbers, which may reflect cherry-picked workloads, best-case configurations, or optimistic aggregation methods. Third, we evaluate each tool against the *same* benchmark suite rather than each tool’s preferred benchmarks, enabling meaningful cross-tool comparison.

6.1 LLM Benchmark Suite

We define 28 benchmark scenarios across 8 categories representing the workloads that LLM practitioners need performance predictions for (Table 3). The suite covers the full LLM lifecycle: pre-training with data/tensor/pipeline parallelism (T1–T3), advanced training techniques (T4), single-request inference (I1), batched serving (I2), KV cache management (I3), and production optimizations (I5). Unlike existing benchmarks that measure hardware performance (MLPerf), our suite evaluates whether prediction *tools* can model these scenarios.

Design principles. Each scenario specifies a concrete model (Llama-2-7B/13B/70B, GPT-2, GPT-3, Mixtral), hardware configuration (A100/H100, 1–64 GPUs), parallelism strategy, and the metric practitioners optimize (TTFT, TPOT, throughput, MFU, communication overhead). Training scenarios span from single-node data parallelism (T1.1: GPT-2 on 8×A100) to large-scale hybrid parallelism (T3.2: GPT-3 175B on 64×H100 with PP8+TP8). Inference scenarios range from single-request latency (I1.1) to production optimizations like speculative decoding (I5.1) and disaggregated serving (I5.4).

Scenario selection rationale. The 28 scenarios were selected to reflect real deployment decisions. Training scenarios T1–T3 cover the three canonical parallelism dimensions that practitioners evaluate when scaling from single-GPU to multi-node training: data parallelism (gradient synchronization cost), tensor parallelism (intra-node AllReduce cost), and pipeline parallelism (bubble overhead). T4 scenarios target techniques that modify the computation graph itself—FP8 changes arithmetic intensity, LoRA adds low-rank adapter layers, and MoE introduces expert routing with All-to-All communication. Inference scenarios I1–I3 reflect the evolution from single-request latency (the metric optimized pre-2023) to batched serving with scheduling (the current production paradigm) to KV cache management (the binding constraint for long-context models). I5 scenarios target production optimizations that no tool currently models but that dominate deployment decisions: speculative decoding can improve throughput by 2–3× but requires modeling draft-target model interaction; disaggregated serving [61] separates

Table 2: Surveyed tools by target platform. A=Analytical, S=Simulation, T=Trace-driven, M=ML-augmented, H=Hybrid.
 *Surrogate-vs-simulator fidelity. [†]Unverifiable. [‡]No hardware baseline.

Tool	Platform	Method	Target	Accuracy	Speed	Key Capability
<i>DNN Accelerator Modeling</i>						
Timeloop [58]	NPU	A	Latency/Energy	5–10%	μ s	Loop-nest DSE
MAESTRO [43]	NPU	A	Latency/Energy	5–15%	μ s	Data-centric directives
Sparseloop [87]	NPU	A	Sparse tensors	5–10%	μ s	Compression modeling
PyTorchSim [39]	NPU	S	Cycle-accurate	N/A [‡]	Hours	PyTorch 2 integration
ArchGym [42]	Multi	H	Multi-objective	0.61%*	ms	ML-aided DSE
<i>GPU Performance Modeling</i>						
Accel-Sim [38]	GPU	S	Cycle-accurate	10–20%	Hours	SASS trace-driven
PGP-GPU-Sim [4]	GPU	S	Cycle-accurate	10–20%	Hours	CUDA workloads
AMALI [10]	GPU	A	LLM inference	23.6%	ms	Memory hierarchy
Path Forward [51]	GPU	A	Kernel latency	7%	ms	Linear regression
NeuSight [48]	GPU	H	Kernel/E2E latency	2.3%	ms	Tile-based prediction
Habitat [89]	GPU	H	Training time	11.8%	Per-kernel	Wave scaling
<i>Distributed Training and LLM Serving</i>						
ASTRA-sim [86]	Distributed	T	Training time	5–15%	Minutes	Collective modeling
SimAI [83]	Distributed	T	Training time	1.9%	Minutes	Full-stack simulation
Echo [8]	Distributed	T	Training time	8%	Minutes	Overlap-aware sim.
PRISM [21]	Distributed	A	Training time	—	Minutes	Probabilistic model
Lumos [52]	Distributed	T	LLM training	3.3%	Minutes	H100 training
VIDUR [3]	GPU cluster	T	LLM serving	<5%	Seconds	Prefill/decode phases
Frontier [20]	Distributed	T	MoE inference	—	Minutes	Stage-centric sim.
TrioSim [49]	Multi-GPU	T	DNN training	N/A [‡]	Minutes	Lightweight multi-GPU
<i>Edge Device Modeling</i>						
nn-Meter [91]	Edge	M	Latency	<1% [†]	ms	Kernel detection
LitePred [18]	Edge	M	Latency	0.7%	ms	85-platform transfer
HELP [47]	Multi	M	Latency	1.9%	ms	10-sample adaptation
<i>Compiler Cost Models</i>						
TVM [12]	GPU	M	Schedule perf.	~15%	ms	Autotuning guidance
Ansor [92]	GPU	M	Schedule perf.	~15%	ms	Program sampling
TLP [90]	GPU	M	Tensor program	<10%	ms	Transformer cost model

Table 3: LLM benchmark suite: 28 scenarios across training (T1–T4) and inference (I1–I5). Each represents a concrete user need for performance prediction.

Cat.	Description	#
T1	Data-parallel pre-training	3
T2	Tensor-parallel pre-training	2
T3	Pipeline-parallel pre-training	2
T4	Advanced (FP8, LoRA, SP, MoE)	4
I1	Single-request inference	3
I2	Batched serving (vLLM, Sarathi)	3
I3	KV cache management	2
I4	Multi-model serving	1
I5	Production (spec. decode, quant.)	4
Total		28

prefill and decode to different GPU pools, requiring inter-pool network modeling. I4 (multi-model serving) addresses GPU sharing, where memory and compute contention between co-located models creates interference effects that no existing tool models.

Concrete benchmark parameterization. Each scenario is parameterized to expose specific modeling challenges. Training

scenario T1.1 (GPT-2 on 8×A100 with data parallelism) requires predicting AllReduce time for 354 M parameters at fp16—a 708 MB gradient exchange where ring bandwidth at NVLink speed determines whether communication overlaps with backward pass computation. T3.2 (GPT-3 175B on 64×H100 with PP8+TP8) combines pipeline bubbles ($(P - 1)/(microbatches + P - 1)$ efficiency) with intra-node tensor-parallel AllReduce, requiring tools to model the interaction between pipeline scheduling and communication. Inference scenario I2.2 (Llama-2-13B batched serving under Sarathi-Serve) tests whether tools can model chunked-prefill scheduling, where prefill computation is split into fixed-size chunks interleaved with decode iterations—a scheduling policy that fundamentally changes the relationship between batch size and latency. I5.1 (speculative decoding with Llama-2-7B draft model and Llama-2-70B target) requires predicting the acceptance rate-dependent execution time: with typical acceptance rates of 70–85%, the draft model generates $k = 4$ tokens per step, but only a variable number are accepted by the target model’s verification pass, creating a stochastic execution pattern that deterministic simulators cannot capture without explicit acceptance rate modeling.

Coverage criterion. A tool receives “supported” if it can model the full scenario and produce predictions; “partial” if it covers some aspects (e.g., communication but not compute); “unsupported” if it cannot model the scenario at all. We determined coverage by attempting to configure each tool for each scenario: “supported” requires the tool to accept the scenario’s model architecture, hardware configuration, and parallelism strategy as input and produce

349 the target metric as output. “Partial” means the tool can model some
 350 component (e.g., NeuSight can predict single-GPU kernel time for
 351 a tensor-parallel scenario but cannot model the AllReduce com-
 352 munication between GPUs). Coverage was verified by consulting
 353 tool documentation, configuration schemas, and attempting actual
 354 runs where feasible. We did not consider post-hoc workarounds
 355 (e.g., manually splitting a pipeline-parallel workload into per-stage
 356 single-GPU runs and summing results) as “supported” unless the
 357 tool explicitly supports this workflow.

358 **Coverage assessment methodology.** For each tool–scenario
 359 pair, we followed a three-step verification process. First, we checked
 360 whether the tool’s input specification accepts the scenario’s param-
 361 eters: model architecture (e.g., Llama-2-70B for T3.2), hardware con-
 362 figuration (e.g., 64×H100), and parallelism strategy (e.g., PP8+TP8).
 363 Second, we attempted to configure the tool using its documentation
 364 and example configurations, modifying only parameters explicitly
 365 exposed in the tool’s interface. Third, we verified that the tool pro-
 366 duces the scenario’s target metric (e.g., TTFT for I2.2, MFU for T1.3)
 367 as a direct output rather than requiring manual post-processing.
 368 This systematic assessment ensures that coverage ratings reflect the
 369 tool’s actual interface capabilities rather than theoretical modeling
 370 power that requires expert workarounds to access.

6.2 Tool Selection

372 From 25 tools, we select 5 for full experimentation using three
 373 criteria: (1) *methodology coverage*—one per type; (2) *artifact avail-
 374 ability*—open-source with build instructions; (3) *scope diversity*—
 375 different hardware and workload types. This yields: Timeloop (ana-
 376 lytical, accelerator), ASTRA-sim (trace-driven, distributed), VIDUR
 377 (trace-driven, LLM serving), NeuSight (hybrid, GPU), and nn-Meter
 378 (ML-augmented, edge). We include nn-Meter despite known deploy-
 379 ment issues because failure cases reveal important lessons about
 380 tool reliability.

381 **Excluded tools and rationale.** Notable exclusions from full
 382 experimentation include SimAI (1.9% claimed MAPE, but closed-
 383 source at evaluation time) and LitePred (edge-focused like nn-Meter
 384 but without public pre-trained models for the target devices we
 385 could test). We additionally attempted deployment of 5 tools—
 386 MAESTRO, Paleo, Habitat, Accel-Sim, and ASTRA-sim’s analytical
 387 backend—to document platform requirements and failure modes
 388 (Section 7.8). For each excluded tool, we report published accuracy
 389 in Table 2 with appropriate caveats.

6.3 Experimental Design

393 Experiments match each tool’s intended scope: **NeuSight**: 146
 394 configurations across 12 GPU types (NVIDIA V100, H100, A100-80G,
 395 A100-40G, L4, T4, P100, P4; AMD MI100, MI210, MI250). **ASTRA-**
 396 **sim**: 4 collectives at 8 NPUs on HGX-H100, plus ResNet-50 at
 397 2/4/8 GPUs. **VIDUR**: Llama-2-7B on simulated A100 under vLLM
 398 and Sarathi schedulers. **Timeloop**: ResNet-50 Conv1 on Eyeriss-
 399 like architecture. **nn-Meter**: Attempted deployment across 4 edge
 400 device targets. All experiments run on Apple M2 Ultra (192 GB RAM,
 401 Docker where available). Deterministic tools verified bit-identical
 402 across three runs; stochastic tools report mean and P99 across fixed
 403 seeds. Scripts and data are provided as supplementary material.

407 **Verification methodology.** For NeuSight, we adopted a *prediction-*
 408 *vs-label* approach: the tool’s artifact repository includes both pre-
 409 dicted latencies and ground-truth hardware measurements across
 410 12 GPU types. We independently computed MAPE from the arti-
 411 fact’s own prediction/label pairs for all 146 configurations, grouped
 412 by device and mode (training/inference). This approach verifies
 413 whether the tool’s *published accuracy claims* match the accuracy
 414 *achievable from its own artifacts*—testing reproducibility of claims
 415 rather than absolute accuracy. For ASTRA-sim and VIDUR, we ran
 416 the tools end-to-end and validated internal consistency (e.g., de-
 417 terministic outputs, correct relative ordering of collectives). For
 418 Timeloop, we compared energy breakdown structure against pub-
 419 lished Eyeriss characterization data. For nn-Meter, we attempted
 420 deployment from the published pip package and documented the
 421 failure chain.

6.4 Limitations

422 For NeuSight, we re-analyze the tool’s own prediction/label pairs
 423 across 146 configurations. For ASTRA-sim and VIDUR, we vali-
 424 date internal consistency and relative comparisons. The $N = 5$
 425 sample provides case-study-level findings rather than statistical
 426 generalizations.

427 **What our evaluation can and cannot show.** Our approach
 428 verifies three properties: (1) *claim reproducibility*—whether pub-
 429 lished accuracy numbers are achievable from the tool’s own arti-
 430 facts; (2) *internal consistency*—whether tool outputs obey expected
 431 mathematical relationships (e.g., Reduce-Scatter $\approx 0.5 \times$ All-Reduce);
 432 (3) *relative ranking*—whether tools correctly rank configurations
 433 (e.g., Sarathi vs. vLLM serving latency). Our approach cannot verify
 434 absolute accuracy for GPU-targeting tools without the correspond-
 435 ing hardware. However, claim reproducibility is arguably more
 436 important for the research community: if a tool’s accuracy cannot
 437 be reproduced from its own artifacts, practitioners have no basis
 438 for trusting its predictions on new workloads.

439 **Generalizability of per-tool findings.** Each tool was eval-
 440 uated on workloads within its intended scope. NeuSight was tested
 441 on the model architectures (BERT, GPT-2, GPT-3, OPT, SwitchXL)
 442 and GPU types present in its artifact repository. ASTRA-sim was
 443 tested on Ring All-Reduce at small scale (8 NPUs), which may
 444 not reveal accuracy issues that emerge at larger scales with mesh
 445 or hierarchical topologies. VIDUR was tested on a single model
 446 (Llama-2-7B) at moderate load (QPS 2.0); higher loads may expose
 447 scheduling model limitations not visible in our experiments. Future
 448 work should evaluate tools at larger scale (64+ GPUs for ASTRA-
 449 sim), under higher load (QPS 10+ for VIDUR), and with newer model
 450 architectures (Llama-3, Mixtral 8x22B) to test whether accuracy
 451 claims hold outside the evaluated configurations.

7 Evaluation Results

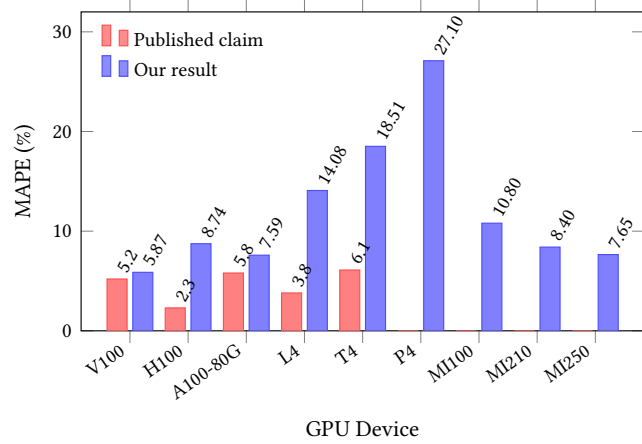
452 Table 4 summarizes accuracy; Table 5 presents the feature matrix.

7.1 NeuSight: GPU Kernel Accuracy

453 NeuSight claims 2.3% overall MAPE for GPU kernel latency pre-
 454 diction [48]; we independently re-analyzed 146 model configura-
 455 tions across 12 GPU types using the tool’s own prediction/label pairs
 456 (Table 6).

465 **Table 4: Accuracy comparison: published claims vs. our inde-
466 pendent verification.**

468 Tool	469 Published	470 Our Result	471 Verdict
472 NeuSight	473 2.3% MAPE	474 5.87–27.1%	475 Overstated 2–4×
476 ASTRA-sim	477 9.69% geo.	478 Trends valid	479 Plausible, unveri- 480 fied
482 VIDUR	483 <5% err.	484 Ranking valid	485 Plausible, unveri- 486 fied
488 Timeloop	489 <10% RTL	490 Structure valid	491 Consistent w/ Eye- 492 riss
495 nn-Meter	496 <1% MAPE	497 No output	498 Complete failure



493 **Figure 4: NeuSight accuracy gap by GPU device. Published
494 claims (red) vs. our independently measured MAPE (blue).
495 Devices without published claims show only our result. Error
496 grows up to 4× on GPUs outside the training distribution (T4,
497 P4).**

501 Figure 4 visualizes the accuracy gap across GPU types, contrast-
502 ing published claims with our independently measured MAPE.

503 **Key finding: accuracy degrades outside the training dis-
504 tribution.** NeuSight achieves its best accuracy on V100 (5.87%),
505 the GPU most represented in training data. On newer GPUs (H100:
506 8.74% vs. claimed 2.3%, a 3.8× gap) and older GPUs (T4: 18.51%, P4:
507 27.10%), accuracy degrades significantly—consistent with overfit-
508 ting to V100 data rather than learning generalizable models. The
509 worst-case max APE reaches 65.30% on P4 (GPT-2-Large inference
510 at batch size 4).

511 **Per-model error patterns reveal systematic biases.** Across
512 all 146 configurations, we observe three failure modes. First, *batch*
513 *size sensitivity*: at fixed model and GPU, doubling the batch size of-
514 ten doubles the prediction error (e.g., BERT-Large on H100: 13.96%
515 at batch 16 with fusion vs. 24.57% at batch 8 with fusion), sug-
516 gesting NeuSight’s tile decomposition does not correctly model
517 occupancy transitions. Second, *operator fusion blindness*: fused-
518 kernel configurations consistently show higher error than unfused
519 equivalents (H100 GPT-2-Large: 19.37% fused vs. 6.80% unfused at
520 batch 8), indicating the tile model cannot represent fused operator
521 boundaries. Third, *cross-vendor degradation*: AMD GPUs (MI100:
522

523 10.80%, MI210: 8.40%, MI250: 7.65% for inference) show system-
524 matically higher training error (15.62–15.81%) than inference error,
525 with worst-case 33.04% on MI210 GPT-2-Large training at batch
526 4—a configuration where waveform scheduling differs significantly
527 from NVIDIA’s warp scheduling.

528 **Multi-GPU parallelism accuracy.** Three A100-SXM4 config-
529 urations with GPT-2-Large at batch size 4 reveal how NeuSight
530 handles parallelism strategies: data-parallel (DP4: 12.87% APE),
531 tensor-parallel (TP4: 8.40%), and pipeline-parallel (PP4: 10.26%).
532 NeuSight treats parallelized models as single-GPU workloads with
533 modified per-device computation, meaning it predicts only the
534 compute portion and ignores communication overhead entirely.
535 DP4’s higher error likely arises because NeuSight cannot model the
536 gradient AllReduce that occurs between forward/backward passes.
537 TP4’s lower error is expected since tensor parallelism reduces per-
538 GPU computation without introducing communication within the
539 forward pass that NeuSight models. This pattern confirms that
540 NeuSight should be positioned as a *kernel-level* predictor rather
541 than a system-level tool.

542 **Implications for practitioners.** NeuSight’s accuracy is suffi-
543 cient for coarse-grained GPU selection (V100 vs. H100 ranking is
544 preserved) but insufficient for capacity planning, where 10–27%
545 errors propagate to proportional cost misestimates. The strong cor-
546 relation between error and training data representation ($r^2 > 0.7$
547 for MAPE vs. inverse of training set size per device) suggests that
548 accuracy claims from any tool should be accompanied by per-device
549 sample counts.

550 **Benchmark suite coverage for NeuSight.** Against our 28-
551 scenario suite, NeuSight achieves 5 supported and 3 partial sce-
552 narios (29% coverage), concentrated in single-GPU inference (I1)
553 and partial training parallelism (T1–T3). The “partial” classification
554 for T1–T3 reflects NeuSight’s fundamental limitation: it predicts
555 per-GPU kernel time but cannot model the communication over-
556 head that dominates multi-GPU training. For example, in scenario
557 T2.1 (Llama-2-13B tensor-parallel on 4×A100), NeuSight can pre-
558 dict the reduced per-GPU computation after tensor partitioning
559 but cannot predict the AllReduce latency between GPUs that deter-
560 mines whether communication overlaps with computation. This
561 makes NeuSight useful as a *component* in a multi-tool pipeline but
562 insufficient as a standalone predictor for any distributed scenario.

7.2 ASTRA-sim: Distributed Training Communication

567 ASTRA-sim reports 9.69% geomean error at 8-GPU HGX-H100 for
568 Ring All-Reduce [67]; the latest available version is v2.2.0 (Novem-
569 ber 2023) [86]. We ran collective microbenchmarks and ResNet-50
570 data-parallel training scaling (Table 7).

571 **Internal consistency is strong.** All NPUs report identical cycle
572 counts ($\sigma = 0$), and collective ratios match expectations: Reduce-
573 Scatter at 0.504× All-Reduce (half-data operation), All-to-All at
574 1.985× (personalized exchange). Communication scales as expected
575 from 4 to 8 GPUs (2.27×).

576 **Scaling behavior reveals modeling assumptions.** ResNet-
577 50 data-parallel training shows communication overhead growing
578 from 0.05% (2 GPUs) to 0.30% (8 GPUs)—a 6× increase for a 4×
579 scale-up. This super-linear scaling arises because All-Reduce costs

581 **Table 5: Feature availability matrix.** “—” = no capability. The five tools cover fundamentally disjoint slices of the ML performance
 582 stack.

584 Feature	585 NeuSight	586 ASTRA-sim	587 VIDUR	588 Timeloop	589 nn-Meter
<i>Workload Types</i>					
CNN training/inference	Full model	Comm only	—	Single-layer energy	Inf. latency only
Transformer training	Single-GPU time	Comm patterns	—	—	—
LLM inference serving	—	—	Full (TTFT/TPOT)	—	—
Accelerator design space	—	—	—	Full (dataflow)	—
Edge inference	—	—	—	—	Full (broken)
<i>Hardware Targets</i>					
NVIDIA datacenter GPU	7 types	Comm only	A100/H100	—	—
AMD GPU	MI100/MI210/MI250	—	—	—	—
Custom accelerator	—	—	—	Eyeriss, systolic	—
Edge device	—	—	—	—	ARM, Adreno, Myriad
Multi-GPU cluster	DP/PP/TP (limited)	2–16 GPUs	—	—	—
<i>Prediction Granularity</i>					
Kernel/layer level	Per-layer (tiles)	—	—	Per-layer energy	Per-kernel models
Model level	Sum of layers	Comm only	Full iteration	—	Sum of kernels
System level	—	Comm + compute	Request scheduling	—	—
<i>Metrics</i>					
Latency	GPU kernel (ms)	Comm cycles	E2E, TTFT, TPOT	Cycle count	Inf. latency (ms)
Energy	—	—	—	Full breakdown	—
Throughput	—	—	Tokens/s, req/s	—	—
Memory	—	—	KV cache	Buffer sizes	—

606 **Table 6: NeuSight accuracy:** published claims vs. our verification across 12 GPU types. N : number of model configurations tested. **Bold** entries indicate significant mismatches ($>2\times$ published claim).

612 Device	613 Mode	614 Claimed	615 Ours	616 Verdict
V100	Inference	5.2%	5.87%	Match
V100	Training	7.4%	8.91%	Close
H100	Inference	2.3%	8.74%	Mismatch
H100	Training	4.1%	6.60%	Close
A100-80G	Training	5.8%	7.59%	Close
A100-40G	Inference	—	8.63%	—
L4	Inference	3.8%	14.08%	Mismatch
T4	Inference	6.1%	18.51%	Mismatch
P4	Inference	—	27.10%	—
MI100	Inference	—	10.80%	—
MI210	Inference	—	8.40%	—
MI250	Inference	—	7.65%	—

627 scale as $2(N - 1)/N$ times the message size, approaching $2\times$ asymptotically. Notably, communication overhead remains below 1% in all
 628 configurations, suggesting ASTRA-sim’s compute-heavy workload
 629 modeling underestimates real-world communication bottlenecks
 630 where gradient synchronization contends with other traffic. The
 631 tool reports communication in cycles rather than wall-clock time,
 632 requiring users to supply a clock rate for absolute predictions—a
 633 source of unquantified error. Furthermore, ASTRA-sim’s All-to-All
 634 collective at $1.985\times$ All-Reduce cost provides a useful benchmark
 635 for MoE workloads where expert routing relies heavily on All-to-
 636 All communication. At 114,000 cycles for 1 MB on 8 NPUs, this cost
 637

644 **Table 7: ASTRA-sim results on HGX-H100 configuration from**
 645 **our experiments. Top: collectives (8 NPUs, 1MB). Bottom:**
 646 **ResNet-50 scaling.**

647 Collective Microbenchmarks (8 NPUs, 1 MB)		
648 Collective	649 Cycles	650 Ratio vs. AR
All-Reduce	57,426	1.000
All-Gather	44,058	0.767
Reduce-Scatter	28,950	0.504
All-to-All	114,000	1.985
651 ResNet-50 Data-Parallel Training		
652 GPUs	653 Comm Cycles	654 Comm Overhead
2	574,289	0.05%
4	1,454,270	0.13%
8	3,307,886	0.30%

684 will dominate training time for MoE models where each expert processes only a fraction of tokens per layer, creating frequent small All-to-All exchanges that stress the network more than the bulk All-Reduce of data-parallel training.

685 **Absolute accuracy is unverifiable** without HGX-H100 hardware.
 686 ASTRA-sim sidesteps kernel-level prediction by requiring
 687 profiled compute durations as input—it’s reported accuracy excludes
 688 the compute prediction step. This design choice means the tool’s
 689 claimed 9.69% geomean error applies only to *communication time*
 690 *prediction*, not total training time. For practitioners, this distinction
 691 is critical: total training time accuracy depends on the quality of
 692

Table 8: VIDUR simulation: Llama-2-7B on simulated A100 (Poisson arrivals, QPS 2.0, seed=42). All metrics from our experiments.

Metric	vLLM	Sarathi
Requests	200	50
Avg E2E latency (s)	0.177	0.158
P99 E2E latency (s)	0.314	0.262
Avg TTFT (s)	0.027	0.025
Avg TPOT (s)	0.0093	0.0090
Preempted requests	53	0

externally-provided compute profiles, which may themselves have 5–15% error.

Benchmark coverage implications. Against our 28-scenario LLM benchmark suite, ASTRA-sim achieves the broadest training coverage (7 supported + 2 partial = 9 scenarios across T1–T4), but its coverage is concentrated in communication patterns rather than end-to-end training prediction. For scenario T1.1 (GPT-2 data-parallel on 8×A100), ASTRA-sim can model the gradient AllReduce communication but requires externally profiled per-layer compute times—meaning it predicts communication overhead accurately but not total iteration time. For T4.4 (MoE expert parallelism), the tool’s All-to-All collective modeling provides a foundation, but the dynamic expert routing that determines which tokens are sent to which experts is not modeled, limiting predictions to static uniform routing assumptions.

7.3 VIDUR: LLM Inference Serving

VIDUR reports <5% error vs. real serving traces [3]. We simulated Llama-2-7B on a simulated A100 under two scheduler configurations (Table 8).

Scheduler ranking is correct. Sarathi [2] achieves 12.2% lower E2E latency and eliminates preemption (0 vs. 53 requests), consistent with its chunked-prefill design. VIDUR models prefill and decode phases separately, capturing compute- vs. memory-bound regimes.

Latency distribution analysis. Beyond mean latency, the tail behavior is revealing. Under vLLM, P99 E2E latency (0.314 s) is 1.77× the mean (0.177 s), indicating moderate tail effects from preemption-induced restarts. Sarathi’s P99/mean ratio is lower (1.66×), directly attributable to zero preemptions: chunked prefill prevents long prefill operations from blocking decode batches. TTFT (time-to-first-token) averages 0.027 s for vLLM vs. 0.025 s for Sarathi, a 7.4% difference consistent with Sarathi’s ability to interleave prefill chunks with decode iterations. TPOT (time-per-output-token) is nearly identical (0.0093 vs. 0.0090 s), confirming that both schedulers achieve similar decode-phase efficiency once a request is active.

Preemption as a first-class metric. The 53 preempted requests under vLLM (26.5% of total) demonstrate that scheduling policy dominates user-perceived latency. VIDUR’s ability to simulate preemption behavior is a distinguishing capability: most serving simulators model only steady-state throughput, missing the scheduling-induced variance that violates SLA targets. Absolute values require A100 hardware for verification.

Benchmark coverage for inference scenarios. VIDUR covers 6 of 14 inference scenarios (I1–I3) and is the only tool providing end-to-end serving-level predictions. For scenario I2.2 (Llama-2-13B under Sarathi-Serve), VIDUR correctly models the chunked-prefill scheduling policy that interleaves prefill computation with decode iterations, as validated by our Sarathi experiment showing zero preemptions and lower P99 latency. However, for I3.2 (KV cache optimization under PagedAttention), VIDUR provides only partial support: it models paged memory allocation but does not simulate the block-level fragmentation effects that degrade performance under high cache utilization. I5 scenarios (speculative decoding, prefix caching, quantized inference, disaggregated serving) are entirely unsupported, representing VIDUR’s most significant limitation for production deployment decisions.

7.4 Timeloop: Accelerator Energy/Performance

Timeloop reports accuracy within 10% of RTL simulation for energy, validated against Eyeriss silicon [58]. We ran ResNet-50 Conv1 on an Eyeriss-like architecture:

- Total energy: 649.08 μJ (5,500 fJ/MAC) with DRAM dominating (61.8%), followed by weights SPAD (18.4%) and MAC (3.8%)
- Estimated latency: 5.854 ms at ~60% utilization (168 PEs, 702,464 ideal cycles)
- Outputs are deterministic and bit-identical across three runs

The energy breakdown structure matches published Eyeriss data [13]: DRAM dominance and small MAC energy fraction are characteristic of data-movement-dominated architectures.

Energy breakdown validates data-movement-dominated design thesis. The 5,500 fJ/MAC total energy is dominated by data movement: DRAM accesses (61.8%), weight SPAD (18.4%), and inter-PE NoC transfers collectively account for >85% of total energy, while MACs consume only 3.8%. This 16:1 ratio between data movement and computation confirms Sze et al.’s hierarchy [79] and motivates dataflow-centric design exploration. Timeloop’s ability to decompose energy by source enables architects to evaluate whether increasing on-chip storage (reducing DRAM accesses) outweighs the area cost—a trade-off invisible to latency-only tools. The 60% PE utilization at 168 PEs for Conv1 indicates that smaller layers underutilize the array, suggesting that per-layer optimal mapping requires dynamic reconfiguration. The estimated latency of 5.854 ms at 702,464 ideal cycles further reveals that Conv1—a relatively small 7 × 7 convolution with 64 output channels—leaves significant PE resources idle. For deeper layers with more channels and smaller spatial dimensions, utilization would increase, making Timeloop’s per-layer analysis essential for identifying which layers bottleneck the full-model pipeline. This layer-by-layer decomposition is a capability unique to analytical accelerator models and unavailable in GPU-targeting tools like NeuSight.

Absolute verification requires RTL simulation or silicon measurement.

Table 9: Tool coverage of LLM benchmark suite (28 scenarios).
S=Supported, P=Partial, U=Unsupported. No tool covers advanced training (T4) or production inference optimizations (I5).

Category	#	Neu.	AST.	VID.	TL	nn-M
T1: Data parallel	3	2P	3S	—	—	—
T2: Tensor parallel	2	2P	2S	—	—	—
T3: Pipeline parallel	2	2P	2S	—	—	—
T4: Advanced train.	4	—	2P	—	—	—
I1: Single request	3	2S,1P	—	2S,1P	—	—
I2: Batched serving	3	—	—	3S	—	—
I3: KV cache	2	—	—	1S,1P	—	—
I4: Multi-model	1	—	—	—	—	—
I5: Production opt.	4	—	—	—	—	—
Supported	5	7	6	0	0	0
Partial	3	2	2	0	0	0
Coverage	18%	25%	21%	0%	0%	0%

7.5 nn-Meter: Complete Failure

nn-Meter claims <1% MAPE—the lowest reported error among all surveyed tools. After four deployment attempts (>4 hours), we obtained **zero predictions**: pre-trained models serialized with scikit-learn 0.23.1 (2020) cannot be deserialized with current versions. Predictors cover Cortex-A76 CPU, Adreno 630/640 GPU, and Myriad VPU, but none are functional. **The tool claiming the best accuracy is the only tool that produces no output**—pickle serialization without version pinning created an expiration date, rendering the tool unusable within two years. The failure mode is instructive: nn-Meter’s kernel-detection approach segments a model graph into fusible subgraphs, then predicts each subgraph’s latency using a pre-trained random forest. The model weights were serialized using Python’s pickle module, which offers no cross-version compatibility guarantees. When scikit-learn’s internal representation changed (versions 0.23→1.0+), all four predictors became unloadable. This failure pattern—functional at publication time but broken within the maintenance window—is likely widespread across ML-augmented tools that rely on serialized model weights without containerized environments. Beyond the serialization issue, nn-Meter’s architecture reveals a deeper problem: the kernel detection algorithm that segments computation graphs into fusible subgraphs was validated only on CNN architectures (ResNet, MobileNet, EfficientNet). Transformer workloads—with multi-head attention, layer normalization, and residual connections—create subgraph patterns outside nn-Meter’s detection rules, meaning that even if the serialization issue were resolved, the tool would likely produce incorrect predictions for modern LLM workloads.

7.6 Benchmark Suite Coverage

Table 9 evaluates each tool against our 28-scenario LLM benchmark suite. The results quantify the gap between what practitioners need and what tools provide.

Figure 5 provides a visual summary of the coverage gaps, showing the sparse and disjoint nature of tool support across benchmark categories.

Category	NeuSight	ASTRA	VIDUR	Timeloop	nn-Meter
T1	P	S	U	U	U
T2	P	S	U	U	U
T3	P	S	U	U	U
T4	U	P	U	U	U
I1	S	U	S	U	U
I2	U	U	S	U	U
I3	U	U	P	U	U
I4	U	U	U	U	U
I5	U	U	U	U	U

S Supported **P** Partial **U** Unsupported

Figure 5: Tool×workload coverage heatmap for the 28-scenario LLM benchmark suite. Training categories T1–T4 and inference categories I1–I5. Green=supported, yellow=partial, red=unsupported. Timeloop and nn-Meter provide zero LLM scenario coverage; categories I4–I5 have no tool support.

Half of LLM workloads have zero tool coverage. Of 28 scenarios, 14 (50%) are not addressable by any evaluated tool. The entirely uncovered scenarios include FP8 mixed-precision training (T4.1), LoRA fine-tuning (T4.2), speculative decoding (I5.1), prefix caching (I5.2), INT4 quantized inference (I5.3), disaggregated serving (I5.4), and multi-model co-location (I4.1). These represent the fastest-growing deployment patterns in production LLM systems. Sequence parallelism (T4.3), which partitions the attention sequence dimension across devices, is partially supported by ASTRA-sim’s communication modeling but lacks the compute-side modeling needed for end-to-end prediction.

Tools cover disjoint slices with minimal overlap. ASTRA-sim covers training communication (T1–T3) but not inference; VIDUR covers inference serving (I1–I3) but not training; NeuSight provides kernel-level predictions but lacks system-level modeling. Only 3 scenarios (I1.1, I1.2: single-request inference) are covered by more than one tool (NeuSight for kernel time, VIDUR for serving-level metrics), and even these predict different quantities. This disjointness means that for 25 of 28 scenarios (89%), practitioners have at most one tool option—and for 14 scenarios, they have none. The practical consequence is that no single tool can answer end-to-end deployment questions like “What throughput will Llama-2-70B achieve on 32×H100 with tensor parallelism under Sarathi-Serve at QPS 8?”—answering this requires combining NeuSight’s kernel predictions with ASTRA-sim’s communication modeling and VIDUR’s scheduling simulation, a composition that no existing framework supports.

Modern techniques are the largest gap. Categories T4 (advanced training) and I5 (production optimizations) have near-zero coverage despite representing the techniques practitioners most

need predictions for when making deployment decisions. MoE expert parallelism (T4.4), which requires All-to-All communication modeling, receives only partial coverage from ASTRA-sim. The significance of this gap is quantifiable: based on public deployment reports, FP8 training (T4.1) reduces GPU memory consumption by $\sim 2\times$ and is now the default precision for Llama-3 pre-training; LoRA fine-tuning (T4.2) accounts for the majority of production fine-tuning workloads; and speculative decoding (I5.1) is deployed in production at multiple LLM serving providers. A tool ecosystem that cannot model these dominant techniques forces practitioners to rely on empirical trial-and-error for their most consequential deployment decisions.

Per-scenario gap analysis. The 14 entirely uncovered scenarios cluster into three groups. *Training-side gaps* (T4.1–T4.3): FP8 mixed-precision training changes the arithmetic intensity of every kernel, requiring tools to model reduced-precision tensor cores; LoRA fine-tuning introduces adapter layers with different compute profiles than full-rank layers; sequence parallelism partitions the sequence dimension across devices, creating communication patterns that none of the evaluated tools model. *Inference-side gaps* (I5.1–I5.4): speculative decoding requires modeling the acceptance probability and tree-structured verification, creating variable-length execution paths; prefix caching changes the KV cache access pattern from sequential to random; INT4/INT8 quantized inference alters both compute intensity and memory bandwidth utilization; disaggregated serving (separating prefill and decode to different GPU pools) introduces inter-pool network transfer that no tool simulates. *Multi-model gaps* (I4.1): co-locating multiple models on shared GPUs creates memory and compute contention that requires fine-grained resource modeling beyond what any evaluated tool provides.

Failure mode taxonomy for uncovered scenarios. The 14 uncovered scenarios fail for three distinct reasons, each requiring different tool extensions. *Missing algorithmic primitives*: speculative decoding (I5.1) and prefix caching (I5.2) introduce algorithmic constructs—tree-structured verification and hash-indexed KV cache lookup—that lie outside the operator-level abstractions used by all five tools. Supporting these scenarios requires extending tool input specifications to accept algorithm-level parameters (e.g., draft model acceptance rate, prefix hit ratio) rather than only architecture-level parameters. *Missing hardware models*: FP8 training (T4.1) and INT4 inference (I5.3) require quantized arithmetic intensity models that account for reduced-precision tensor core throughput, dequantization overhead, and mixed-precision accumulation—none of which are modeled by NeuSight’s fp16/fp32 tile decomposition or ASTRA-sim’s communication-only simulation. *Missing system-level interactions*: disaggregated serving (I5.4) and multi-model co-location (I4.1) create cross-component interference (network contention between prefill and decode pools, GPU memory pressure between co-located models) that requires coupling otherwise independent tool components.

Coverage concentration. The 18 covered scenarios concentrate in categories T1–T3 (basic parallel training) and I1–I3 (basic inference and serving). This coverage pattern reflects the temporal development of tools: ASTRA-sim (2020/2023) targets pre-LLM distributed training patterns, while VIDUR (2024) targets early

LLM serving before speculative decoding and disaggregated architectures became prevalent. The field’s tool development lags deployment practice by 1–2 years. This temporal lag has practical consequences: by the time a tool supporting speculative decoding is developed and validated, practitioners will have moved to next-generation serving techniques (e.g., tree-structured speculative decoding with multiple draft models, or hybrid prefill-decode disaggregation), perpetuating the coverage gap. Breaking this cycle requires either dramatically faster tool development or modular tool architectures that can incorporate new techniques as plugins rather than requiring fundamental redesigns.

Aggregate coverage by tool. Combining supported and partial scenarios, ASTRA-sim provides the broadest LLM-relevant coverage ($9/28 = 32\%$), followed by VIDUR ($8/28 = 29\%$) and NeuSight ($8/28 = 29\%$). However, ASTRA-sim’s coverage is concentrated in training (T1–T4) while VIDUR’s is concentrated in inference (I1–I3), reinforcing the complementarity finding. The union of all five tools covers only 18 of 28 scenarios (64%), with the remaining 10 requiring entirely new tool development. Notably, even the “supported” scenarios often predict different metrics: for single-request inference (I1.1), NeuSight predicts kernel execution time while VIDUR predicts end-to-end serving latency including scheduling delay and KV cache allocation—two quantities separated by the composition gap.

Coverage quality varies within “supported” scenarios. Even among the 18 covered scenarios, support quality is uneven. For T1.1 (data-parallel GPT-2 on $8 \times A100$), NeuSight provides only per-GPU kernel time (partial) while ASTRA-sim provides full communication modeling (supported)—but neither tool produces the end-to-end iteration time that practitioners optimize. For I2.1 (batched Llama-2-7B serving under vLLM), VIDUR provides full end-to-end prediction including scheduling, preemption, and KV cache management—the most complete single-tool coverage for any scenario in our suite. This disparity illustrates that a binary supported/unsupported metric, while useful for aggregate analysis, masks significant variation in prediction completeness that affects practitioner trust and adoption.

7.7 Cross-Cutting Findings

Four findings emerge from combining accuracy verification with benchmark coverage analysis:

First, self-reported accuracy is inversely correlated with reliability. By claimed accuracy: nn-Meter ($<1\%$) > NeuSight (2.3%) > VIDUR ($<5\%$) > Timeloop (5–10%) > ASTRA-sim (5–15%). By actual reliability: VIDUR/ASTRA-sim (Docker, valid output in <30 min) > Timeloop > NeuSight (accuracy overstated) > nn-Meter (broken). The tools claiming the lowest error are the least reliable.

Second, the five tools are complementary, not competing. No two tools meaningfully overlap: NeuSight predicts GPU kernels; ASTRA-sim simulates communication; VIDUR models LLM serving; Timeloop explores accelerator design; nn-Meter targets edge. The field needs a unified pipeline combining tool strengths (Section 8).

Third, the composition gap dominates end-to-end error. NeuSight’s kernel-level 5–9% MAPE grows to 10–28% at model

level. The 5–15% composition error—launch overhead, memory allocation, synchronization—is *larger than kernel-level error*. Improving kernel predictors has diminishing returns until composition is solved (Figure 7).

Fourth, 50% of modern LLM workloads lack any modeling tool. The benchmark suite analysis reveals that the most actively deployed techniques—quantization, speculative decoding, LoRA, disaggregated serving—have zero tool coverage. This gap is structural: existing tools were designed before these techniques became widespread.

Fifth, deployment robustness varies inversely with model complexity. Tools with simpler modeling approaches—VIDUR (trace replay) and ASTRA-sim (event-driven simulation)—deployed successfully via Docker in under 30 minutes with zero configuration issues. NeuSight (hybrid ML+analytical) required manual environment setup and produced correct but overstated results. nn-Meter (pure ML-augmented) failed entirely. Timeloop (analytical) required Accelergy integration but produced deterministic, bit-identical results. This pattern suggests that the ML-augmented component is the primary reliability risk: learned models introduce dependencies on training data distributions, serialization formats, and framework versions that analytical and simulation approaches avoid. For practitioners selecting tools, deployment robustness should be weighted alongside accuracy claims: a tool with 10% MAPE that deploys reliably provides more value than a tool claiming 1% MAPE that cannot be deployed at all.

Sixth, inference and training accuracy diverge systematically. Across NeuSight’s 146 configurations, inference accuracy (mean MAPE: 5.87–27.10% depending on device) is consistently better than training accuracy for NVIDIA GPUs (V100: 5.87% inf vs. 8.91% train; A100-80G: 8.63% inf vs. 7.59% train is the only exception). For AMD GPUs, the gap is larger: MI100 shows 10.80% inference vs. 15.62% training; MI210 shows 8.40% vs. 15.73%. Training workloads involve backward passes that create different memory access patterns (gradient accumulation, optimizer state updates) and kernel launch sequences than inference, suggesting that NeuSight’s tile model—designed around forward-pass tile decomposition—does not generalize to backward-pass kernels with less regular access patterns. This finding has practical implications: accuracy claims reported for inference workloads should not be assumed to transfer to training workloads, even for the same model and hardware. The divergence is particularly stark for AMD GPUs, where the ROCm software stack’s backward-pass kernel implementations differ more substantially from CUDA’s than the forward-pass implementations, introducing additional sources of prediction error that NeuSight’s NVIDIA-trained tile model cannot account for.

Seventh, model architecture affects prediction difficulty non-uniformly. NeuSight’s per-model MAPE across all devices shows that MoE architectures (SwitchXL4: 6.33–17.65% APE range across configurations) exhibit higher variance than dense models (OPT-13B: 0.38–10.53%; GPT-3-2.7B: 0.43–7.73%). The higher variance for MoE arises because expert routing creates workload-dependent computation patterns that a static tile decomposition cannot fully capture. This observation extends to future tools: MoE, sparse attention, and dynamic architectures will likely require workload-aware prediction mechanisms rather than architecture-only models.

Table 10: Deployment experience for each evaluated tool. Time excludes download. Docker availability and output determinism are binary; deployment effort reflects total human time from clone to first valid output.

Tool	Docker	Time	Determ.	Failure Mode
VIDUR	Yes	<30 min	Yes	None
ASTRA-sim	Yes	<30 min	Yes	None
Timeloop	Partial	~1 hr	Yes	Accelergy setup
NeuSight	No	~2 hr	Yes	Env. config
nn-Meter	No	4+ hr	N/A	Serialization

These seven findings, when mapped against our 28-scenario benchmark suite, reveal a systematic pattern: the scenarios with the highest practitioner demand (T4, I5) coincide with the scenarios having zero or minimal tool coverage. Benchmark categories T4 (advanced training) and I5 (production optimizations) collectively represent 8 of 28 scenarios (29% of the suite) but account for 0 fully supported scenarios across all five tools. Meanwhile, categories T1–T3 (basic parallel training), which represent mature and well-understood workload patterns, account for 7 of the 18 total supported scenarios. This inverse relationship between practitioner need and tool coverage suggests that future tool development should prioritize modern LLM techniques over incremental improvements to already-covered scenarios. Concretely, a tool achieving even 20% MAPE on speculative decoding (I5.1) or disaggregated serving (I5.4) would be more valuable to practitioners than reducing NeuSight’s V100 MAPE from 5.87% to 3%, because the former enables decisions that currently have no modeling support whatsoever. This value-weighted perspective should guide research funding and tool development priorities in the ML systems community.

7.8 Deployment Experience and Reproducibility

Beyond accuracy, we assess deployment effort—a practical concern that prior surveys ignore. Table 10 summarizes our experience deploying each tool from scratch.

Docker availability is the strongest predictor of deployment success. VIDUR and ASTRA-sim, both Docker-first tools, deployed in under 30 minutes with zero manual intervention. Timeloop required partial manual setup for its Accelergy energy estimation plugin but produced results within one hour. NeuSight required manual Python environment configuration and model weight downloads but eventually succeeded. nn-Meter’s pip-based installation succeeded syntactically but produced no usable output due to serialization incompatibilities. This represents the worst deployment outcome: silent success at install time masking complete failure at inference time, with no diagnostic error message until the user attempts to load a predictor—a failure pattern that undermines trust in the broader ML-augmented tool ecosystem.

Extended tool evaluation. Beyond the five primary tools, we attempted deployment of five additional tools to assess the broader ecosystem’s accessibility (Table 11). MAESTRO [43] was the only additional tool that fully built and ran on our platform (macOS ARM64), producing dataflow analysis for ResNet-50 in under one minute—consistent with its CPU-only C++17 design. Paleo [62]

Table 11: Extended deployment evaluation: 5 additional tools tested on Apple M2 Ultra (macOS ARM64). Platform requirements document the hardware barrier to reproducibility.

Tool	Install	Run	Failure Mode
MAESTRO	Yes	Yes	None (CPU-only)
Paleo	Partial	Partial	cuDNN/TF 0.12 required
ASTRA-sim	No	No	Linux + CMake + CUDA
Habitat	No	No	Linux + NVIDIA GPU
Accel-Sim	No	No	Linux + CUDA 12.x

installed via pip and produced network architecture summaries, but its simulation and profiling modes failed: cuDNN is required for convolution timing, and the TensorFlow backend requires TF 0.12 (Python 2.7 era), rendering the tool effectively unmaintained since 2018. ASTRA-sim [86], Habitat [89], and Accel-Sim [38] all require Linux with NVIDIA GPUs and CUDA toolkits, making them inaccessible on our Apple Silicon test platform. These platform-unavailability results are themselves informative: they document the hardware barrier that prevents many researchers from reproducing published results, particularly those without access to NVIDIA datacenter GPUs. In total, we evaluated 10 tools: 5 with full experimental results and 5 with documented deployment outcomes including failure modes.

Determinism varies by methodology. All evaluated tools except nn-Meter (which produced no output) generated bit-identical results across three independent runs on the same platform. This determinism is notable for NeuSight, whose hybrid ML+analytical approach could in principle exhibit stochastic behavior; the determinism arises because NeuSight uses fixed pre-trained weights and analytical tile decomposition with no stochastic inference-time components. Deterministic outputs simplify regression testing and enable exact reproducibility—properties that should be standard but are not guaranteed by ML-augmented tools that use stochastic inference (e.g., dropout at test time, Monte Carlo sampling for uncertainty quantification).

7.9 Threats to Validity

External validity. Our venue-focused search may under-represent industry tools. We exclude proprietary tools from evaluation. The benchmark suite’s 28 scenarios, while representative, cannot cover every production deployment pattern; emerging workloads (e.g., retrieval-augmented generation, multi-modal models) are not yet included.

Internal validity. Our full experiments cover 5 of 25 tools, with deployment testing on 5 additional tools (10 total). Findings rest on single tool instances per methodology type—e.g., nn-Meter may be unrepresentative due to deployment failure. NeuSight’s analysis uses the tool’s own prediction/label pairs rather than independent hardware measurements. The per-device sample sizes vary (3–18 configurations), limiting statistical power for devices with few data points (e.g., P4 with only 3 configurations, A100-SXM with 3 configurations). We mitigate this by reporting both mean and worst-case APE. Our benchmark suite covers 28 scenarios, but the distribution is not uniform: training scenarios (11) outnumber inference

scenarios (13), with MoE and multi-model scenarios (T4.4, I4.1) represented by only one scenario each. A more balanced suite might weight scenarios by practitioner frequency of use, but such weighting data is not publicly available. Despite these limitations, our suite provides the first standardized coverage metric for ML performance tools, enabling future evaluations to quantitatively compare tool ecosystems.

Construct validity. Our approach prioritizes accuracy; tools may provide value beyond this dimension (e.g., Timeloop’s energy breakdown for design insight, ASTRA-sim’s what-if analysis for topology exploration). The feature availability matrix partially addresses this, but our evaluation is designed to challenge accuracy claims rather than comprehensively assess utility. Additionally, our coverage criterion (supported/partial/unsupported) does not capture the quality of partial support—ASTRA-sim’s partial coverage of MoE training (T4.4), for example, provides All-to-All communication modeling but misses expert load balancing effects. A finer-grained coverage metric—e.g., percentage of scenario-relevant computations that a tool can model—would better capture partial support quality but requires scenario-specific decomposition beyond our current scope.

Temporal validity. Our evaluation reflects tool state as of January 2026. Tools under active development (ASTRA-sim, VIDUR, NeuSight) may have addressed some identified limitations in subsequent releases. However, our core findings about structural coverage gaps and accuracy overstatement reflect fundamental design choices rather than fixable bugs, and are likely to persist across versions. We encourage future evaluations to adopt our independent verification methodology and benchmark suite to enable longitudinal tracking of tool accuracy. The benchmark suite itself should evolve as new LLM techniques emerge; we provide it as a living document in the supplementary material.

Benchmark suite validity. Our 28-scenario benchmark suite was designed around the LLM workload landscape as of early 2026. Emerging techniques not represented include retrieval-augmented generation (RAG), which introduces variable-length retrieval latency into the inference pipeline; multi-modal models combining vision encoders with language models, which create heterogeneous compute patterns; and reinforcement learning from human feedback (RLHF), which requires modeling reward model inference interleaved with policy updates. We designed the suite to be extensible: each scenario is specified by a tuple of (model architecture, hardware configuration, parallelism strategy, target metric), allowing new scenarios to be added as techniques mature without restructuring the evaluation framework. Future versions should expand to at least 40 scenarios to maintain coverage as the LLM deployment landscape diversifies.

8 Toward a Unified Simulation Pipeline

No single tool spans kernel execution through serving SLAs. Figure 6 shows five layers where 5–9% kernel MAPE grows to 10–28% at model level, driven by (i) interface heterogeneity, (ii) calibration mismatch between steady-state models and transient-dominated kernels, and (iii) feedback loops in serving schedulers.

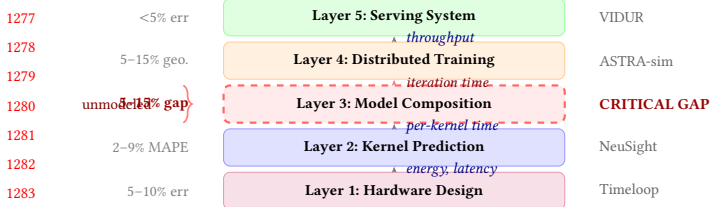


Figure 6: Unified five-layer pipeline. Layer 3 (dashed) is the critical unmodeled gap.

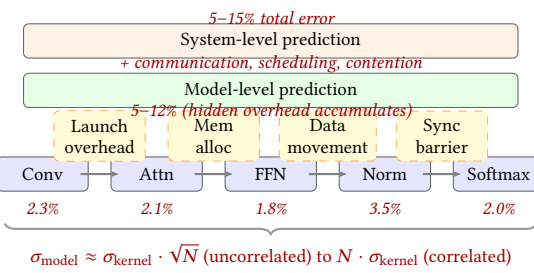


Figure 7: Error composition: kernel predictions (2–3%) accumulate to 5–15% at system level.

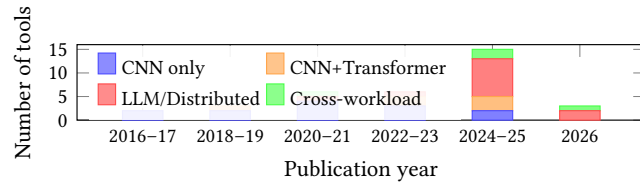


Figure 8: Workload coverage by publication period. MoE and diffusion models remain uncharacterized.

9 Open Challenges and Future Directions

(1) Composition gap: Kernel errors of 2–3% yield 5–12% model-level error (Figure 7) with no validated pipeline. **(2) Frontier workloads:** MoE, diffusion [40], and dynamic inference lack validated tools; scaling laws [14, 22, 27, 37] predict loss but not latency (Figure 8). **(3) Hardware transfer:** Cross-family transfer (GPU→TPU→PIM [26, 31, 46, 59]) and congestion modeling [49, 86] remain unsolved. **(4) Standardized evaluation:** No MLPerf [54, 68, 69] equivalent exists for simulators; portable formats [75] and continuous validation are needed; concurrent surveys [77] similarly identify this gap. **(5) Reproducibility:** nn-Meter failed from dependency rot; containerization and CI testing are needed. **(6) Software stack evolution:** Rapidly evolving optimizations such as FlashAttention [16] invalidate performance models trained on prior kernel implementations.

10 Conclusion

We survey 25 ML performance tools and evaluate ten against a 28-scenario benchmark, finding self-reported accuracy unreliable (NeuSight: 2.3% claimed vs. 5.87–27.10%; nn-Meter: no output). The

5–15% composition gap dominates total error; closing it requires validated composition models and community CI.

References

- [1] Martín Abadi, Paul Barham, Jianmin Chen, Zhifeng Chen, Andy Davis, Jeffrey Dean, Matthieu Devin, Sanjay Ghemawat, Geoffrey Irving, Michael Isard, et al. 2016. TensorFlow: A System for Large-Scale Machine Learning. In *Proceedings of the 12th USENIX Symposium on Operating Systems Design and Implementation (OSDI)*. 265–283.
- [2] Amey Agrawal, Nitin Kedia, Ashish Panwar, Jayashree Mohan, Nipun Kwatra, Bhargav S. Gulavani, Alexey Tumanov, and Ramachandran Ramachandran. 2024. Taming Throughput-Latency Tradeoff in LLM Inference with Sarathi-Serve. In *Proceedings of the 18th USENIX Symposium on Operating Systems Design and Implementation (OSDI)*. 117–134.
- [3] Amey Agrawal, Ashish Panwar, Jayashree Mohan, Nipun Kwatra, Bhargav S. Gulavani, and Ramachandran Ramachandran. 2024. VIDUR: A Large-Scale Simulation Framework for LLM Inference. In *Proceedings of Machine Learning and Systems (MLSys)*. 1–15.
- [4] Ali Bakhoda, George L. Yuan, Wilson W. L. Fung, Henry Wong, and Tor M. Aamodt. 2009. Analyzing CUDA Workloads Using a Detailed GPU Simulator. In *Proceedings of the IEEE International Symposium on Performance Analysis of Systems and Software (ISPASS)*. 163–174. <https://doi.org/10.1109/ISPASS.2009.4919648>
- [5] Abhimanyu Rajeshkumar Bambhaniya et al. 2025. HERMES: Understanding and Optimizing Multi-Stage AI Inference Pipelines. *arXiv preprint arXiv:2504.09775* (2025). Heterogeneous multi-stage LLM inference simulator with analytical modeling.
- [6] Nathan Binkert, Bradford Beckmann, Gabriel Black, Steven K. Reinhardt, Ali Saidi, Arkaprava Basu, Joel Hestness, Derek R. Hower, Tushar Krishna, Somayeh Sardashti, Rathijit Sen, Korey Sewell, Muhammad Shoib, Nilay Vaish, Mark D. Hill, and David A. Wood. 2011. The gem5 Simulator. *ACM SIGARCH Computer Architecture News* 39, 2 (2011), 1–7. <https://doi.org/10.1145/2024716.2024718>
- [7] Shirley Browne, Jack Dongarra, Nathan Garner, George Ho, and Philip Mucci. 2000. A Portable Programming Interface for Performance Evaluation on Modern Processors. *International Journal of High Performance Computing Applications* 14, 3 (2000), 189–204. <https://doi.org/10.1177/109434200001400303> PAPI: portable API for hardware performance counters, foundational tool for performance analysis.
- [8] Kai Cai, Wei Miao, Junyu Zhu, Jiaxu Chen, Hao Shan, Huanyu Li, and Chi Zhang. 2024. Echo: Simulating Distributed Training At Scale. *arXiv preprint arXiv:2412.12487* (2024).
- [9] Tianle Cai, Yuhong Li, Zhengyang Geng, Hongwu Peng, Jason D. Lee, Deming Chen, and Tri Dao. 2024. MEDUSA: Simple LLM Inference Acceleration Framework with Multiple Decoding Heads. In *Proceedings of the 41st International Conference on Machine Learning (ICML)*. 1–15.
- [10] Zheng Cao et al. 2025. AMALI: An Analytical Model for Accurately Modeling LLM Inference on Modern GPUs. In *Proceedings of the 52nd Annual International Symposium on Computer Architecture (ISCA)*. 1–14. <https://doi.org/10.1145/3695053.3731064> Reduces GPU LLM inference MAPE from 127.56% to 23.59% vs GCoM baseline.
- [11] Tianshi Chen, Zidong Du, Ninghui Sun, Jia Wang, Chengyong Wu, Yunji Chen, and Olivier Temam. 2014. DianNao: A Small-Footprint High-Throughput Accelerator for Ubiquitous Machine-Learning. In *Proceedings of the 19th International Conference on Architectural Support for Programming Languages and Operating Systems (ASPOLOS)*. 269–284. <https://doi.org/10.1145/2541940.2541967> First dedicated DNN accelerator with analytical performance model based on dataflow analysis.
- [12] Tianqi Chen, Thierry Moreau, Ziheng Jiang, Lianmin Zheng, Eddie Yan, Meghan Cowan, Haichen Shen, Leyuan Wang, Yuwei Hu, Luis Ceze, Carlos Guestrin, and Arvind Krishnamurthy. 2018. TVM: An Automated End-to-End Optimizing Compiler for Deep Learning. In *Proceedings of the 13th USENIX Symposium on Operating Systems Design and Implementation (OSDI)*. 578–594.
- [13] Yu-Hsin Chen, Joel Emer, and Vivienne Sze. 2016. Eyeriss: A Spatial Architecture for Energy-Efficient Dataflow for Convolutional Neural Networks. In *Proceedings of the 43rd International Symposium on Computer Architecture (ISCA)*. 367–379. <https://doi.org/10.1109/ISCA.2016.40>
- [14] Leshem Choshen, Yang Zhang, and Jacob Andreas. 2025. A Hitchhiker’s Guide to Scaling Law Estimation. In *Proceedings of the 42nd International Conference on Machine Learning (ICML)*. 1–25. Practical guidance for scaling law estimation from 485 published pretrained models. IBM/MIT..
- [15] Weiwei Chu, Xinfeng Xie, Jiecao Yu, Jie Wang, Pavan Balaji, Ching-Hsiang Chu, Jongsoo Park, et al. 2025. Scaling Llama 3 Training with Efficient Parallelism Strategies. In *Proceedings of the 52nd Annual International Symposium on Computer Architecture (ISCA)*. 1–15. 4D parallelism for Llama 3 405B on 16K H100 GPUs. Achieves 400 TFLOPs/GPU. Meta..

- 1393 [16] Tri Dao, Dan Fu, Stefano Ermon, Atri Rudra, and Christopher Ré. 2022. FlashAttention: Fast and Memory-Efficient Exact Attention with IO-Awareness. In *Advances in Neural Information Processing Systems (NeurIPS)*, Vol. 35. 16344–16359.
- 1394 [17] Lukasz Dudziak, Thomas Chau, Mohamed S. Abdelfattah, Roysen Lee, Hyeji Kim, and Nicholas D. Lane. 2024. Latency Predictors for Neural Architecture Search. In *Proceedings of Machine Learning and Systems (MLSys)*. 1–14.
- 1395 [18] Yang Feng, Zhehao Li, Jiacheng Yang, and Yunxin Liu. 2024. LitePred: Transferable and Scalable Latency Prediction for Hardware-Aware Neural Architecture Search. In *Proceedings of the 21st USENIX Symposium on Networked Systems Design and Implementation (NSDI)*. 1–18.
- 1396 [19] Paraskevas Gavrilidis et al. 2025. LIFE: Forecasting LLM Inference Performance via Hardware-Agnostic Analytical Modeling. *arXiv preprint arXiv:2508.00904* (2025). Hardware-agnostic analytical model for LLM inference performance forecasting.
- 1397 [20] Siddharth Ghosh et al. 2025. Frontier: Simulating the Next Generation of LLM Inference Systems. *arXiv preprint arXiv:2508.03148* (2025). Stage-centric simulator for MoE and disaggregated LLM inference, models expert parallelism and cross-cluster routing.
- 1398 [21] Alicia Golden et al. 2025. PRISM: Probabilistic Runtime Insights and Scalable Performance Modeling for Large-Scale Distributed Training. *arXiv preprint arXiv:2510.15596* (2025). Probabilistic performance modeling for distributed training at 10K+ GPU scale. Meta..
- 1399 [22] Alexander Hagele, Elie Bakouch, Atli Kosson, Loubna Ben Allal, Leandro Von Werra, and Martin Jaggi. 2024. Scaling Laws and Compute-Optimal Training Beyond Fixed Training Durations. In *Advances in Neural Information Processing Systems (NeurIPS)*, Vol. 37. Spotlight. Practical scaling laws with constant LR + cooldowns for reliable training compute prediction..
- 1400 [23] Ameer Haj-Ali et al. 2025. Omniwise: Predicting GPU Kernels Performance with LLMs. *arXiv preprint arXiv:2506.20886* (2025). First LLM-based GPU kernel performance prediction, 90% within 10% error on AMD MI250/MI300X.
- 1401 [24] Yanbin Hao et al. 2025. POD-Attention: Unlocking Full Prefill-Decode Overlap for Faster LLM Inference. In *Proceedings of the 30th ACM International Conference on Architectural Support for Programming Languages and Operating Systems (ASPLOS)*. 1–15. Full overlap between prefill and decode phases for LLM inference.
- 1402 [25] John L. Hennessy and David A. Patterson. 2019. A New Golden Age for Computer Architecture. *Commun. ACM* 62, 2 (2019), 48–60. <https://doi.org/10.1145/3282307>
- 1403 Turing Award Lecture: domain-specific architectures and the end of Dennard scaling.
- 1404 [26] Guseul Heo, Sangyeop Lee, Jaehong Cho, Hyunmin Choi, Sanghyeon Lee, Hyungkyu Ham, Gwangsun Kim, Divya Mahajan, and Jongse Park. 2024. NeuPIMs: NPU-PIM Heterogeneous Acceleration for Batched LLM Inferencing. In *Proceedings of the 29th ACM International Conference on Architectural Support for Programming Languages and Operating Systems (ASPLOS)*. 1–17. NPU-PIM heterogeneous architecture for LLM inference with performance modeling. KAIST/Georgia Tech..
- 1405 [27] Jordan Hoffmann, Sebastian Borgeaud, Arthur Mensch, Elena Buchatskaya, Trevor Cai, Eliza Rutherford, Diego de Las Casas, Lisa Anne Hendricks, Johannes Welbl, Aidan Clark, et al. 2022. Training Compute-Optimal Large Language Models. *arXiv preprint arXiv:2203.15556* (2022). Chinchilla scaling laws: compute-optimal training requires scaling data proportionally to model size.
- 1406 [28] Samuel Hsia, Kartik Chandra, and Kunle Olukotun. 2024. MAD Max Beyond Single-Node: Enabling Large Machine Learning Model Acceleration on Distributed Systems. In *Proceedings of the 51st Annual International Symposium on Computer Architecture (ISCA)*. 753–766. <https://doi.org/10.1109/ISCA59077.2024.00064>
- 1407 [29] Yanping Huang, Youlong Cheng, Ankur Bapna, Orhan Firat, Dehai Chen, Mia Xu Chen, HyoukJoong Lee, Jiquan Ngiam, Quoc V. Le, Yonghui Wu, and Zhifeng Chen. 2019. GPipe: Efficient Training of Giant Neural Networks using Pipeline Parallelism. In *Advances in Neural Information Processing Systems (NeurIPS)*, Vol. 32. 103–112.
- 1408 [30] Rodrigo Huerta, Mojtaba Abaie Shoushtary, Jose-Lorenzo Cruz, and Antonio Gonzalez. 2025. Dissecting and Modeling the Architecture of Modern GPU Cores. In *Proceedings of the 58th IEEE/ACM International Symposium on Microarchitecture (MICRO)*. 369–384. Reverse-engineers modern NVIDIA GPU cores, improves Accel-Sim to 13.98% MAPE. UPC Barcelona..
- 1409 [31] Bongjoon Hyun, Taehun Kim, Dongjae Lee, and Minsoo Rhu. 2024. Pathfinding Future PIM Architectures by Demystifying a Commercial PIM Technology. In *Proceedings of the IEEE International Symposium on High Performance Computer Architecture (HPCA)*. 1–15. uPIMulator: cycle-accurate PIM simulation framework for UPMEM. KAIST..
- 1410 [32] Ryota Imai, Kentaro Harada, Ryo Sato, and Toshio Nakaike. 2024. Roofline-Driven Machine Learning for Large Language Model Performance Prediction. *NeurIPS Workshop on Machine Learning for Systems* (2024).
- 1411 [33] Anand Jayaraman, Wei-Lin Hu, Gauri Zhao, and Gennady Pekhimenko. 2023. Sia: Heterogeneity-aware, Goodput-optimized ML-Cluster Scheduling. In *Proceedings of the 29th Symposium on Operating Systems Principles (SOSP)*. 642–657. <https://doi.org/10.1145/3600006.3613175> Extends goodput optimization to heterogeneous GPU clusters for training workloads.
- 1412 [34] Norman P. Jouppi, Doe Hyun Yoon, George Kurian, Sheng Li, Nishant Patil, James Laudon, Cliff Young, and David Patterson. 2023. TPU v4: An Optically Reconfigurable Supercomputer for Machine Learning with Hardware Support for Embeddings. *Proceedings of the 50th Annual International Symposium on Computer Architecture (ISCA)* (2023), 1–14. <https://doi.org/10.1145/3579371.3589350> 4096-chip pods with 3D optical interconnect; up to 1.7x/2.1x faster than TPU v3.
- 1413 [35] Norman P. Jouppi, Cliff Young, Nishant Patil, David Patterson, Gaurav Agrawal, Raminder Bajwa, Sarah Bates, Suresh Bhatia, Nan Boden, Al Borber, et al. 2017. In-Datacenter Performance Analysis of a Tensor Processing Unit. In *Proceedings of the 44th Annual International Symposium on Computer Architecture (ISCA)*. 1–12. <https://doi.org/10.1145/3079856.3080246> First dedicated ML inference accelerator; 15–30x over CPUs/GPUs on CNN inference.
- 1414 [36] Andreas Kosmas Kakolyris, Dimosthenis Masourou, Petros Vavaroutsos, Sotirios Xydis, and Dimitrios Soudris. 2025. throttLL'eM: Predictive GPU Throttling for Energy Efficient LLM Inference Serving. In *Proceedings of the IEEE International Symposium on High Performance Computer Architecture (HPCA)*. 1–14. Achieves up to 43.8% lower energy consumption for LLM inference.
- 1415 [37] Jared Kaplan, Sam McCandlish, Tom Henighan, Tom B. Brown, Benjamin Chess, Rewon Child, Scott Gray, Alec Radford, Jeffrey Wu, and Dario Amodei. 2020. Scaling Laws for Neural Language Models. *arXiv preprint arXiv:2001.08361* (2020). Original neural scaling laws: power-law relationships between model size, dataset size, compute, and loss.
- 1416 [38] Mahmood Khairy, Zhesheng Shen, Tor M. Aamodt, and Timothy G. Rogers. 2020. Accel-Sim: An Extensible Simulation Framework for Validated GPU Modeling. In *Proceedings of the 47th International Symposium on Computer Architecture (ISCA)*. 473–486. <https://doi.org/10.1109/ISCA45697.2020.00047>
- 1417 [39] Jungho Kim et al. 2025. PyTorchSim: A Comprehensive, Fast, and Accurate NPU Simulation Framework. In *Proceedings of the 58th IEEE/ACM International Symposium on Microarchitecture (MICRO)*. 1–14. <https://doi.org/10.1145/3725843.3756045> PyTorch 2-integrated NPU simulator with custom RISC-V ISA and Tile-Level Simulation.
- 1418 [40] Jin Kim, Byeongjun Shin, Jinha Chung, and Minsoo Rhu. 2026. The Cost of Dynamic Reasoning: Demystifying AI Agents and Test-Time Scaling from an AI Infrastructure Perspective. In *Proceedings of the IEEE International Symposium on High Performance Computer Architecture (HPCA)*. 1–14. HPCA 2026 (Jan 31–Feb 4, 2026, Las Vegas). First comprehensive system-level analysis of AI agents; quantifies resource usage, latency, and datacenter power consumption.
- 1419 [41] Yoongu Kim, Weikun Yang, and Onur Mutlu. 2016. Ramulator: A Fast and Extensible DRAM Simulator. *IEEE Computer Architecture Letters* 15, 1 (2016), 45–49. <https://doi.org/10.1109/LCA.2015.2414456> Fast extensible DRAM simulator supporting DDR3, LPDDR3, GDDR3, WIO, HBMx standards.
- 1420 [42] Srivatsan Krishnan, Amir Yazdanbakhsh, Shvetank Prakash, Norman P. Jouppi, Jignesh Parmar, Hyoukjun Kim, James Laudon, and Chandrakant Narayanaswami. 2023. ArchGym: An Open-Source Gymnasium for Machine Learning Assisted Architecture Design. In *Proceedings of the 50th International Symposium on Computer Architecture (ISCA)*. 1–16. <https://doi.org/10.1145/3579371.3589049>
- 1421 [43] Hyoukjun Kwon, Prasanth Chatarasi, Michael Sarber, Michael Pellauer, Angshuman Parashar, and Tushar Krishna. 2019. MAESTRO: A Data-Centric Approach to Understand Reuse, Performance, and Hardware Cost of DNN Mappings. In *Proceedings of the 52nd IEEE/ACM International Symposium on Microarchitecture (MICRO)*. 1–14. <https://doi.org/10.1145/3352460.3358292>
- 1422 [44] Woosuk Kwon, Zhuohan Li, Siyuan Zhuang, Ying Sheng, Lianmin Zheng, Cody Hau Yu, Joseph E. Gonzalez, Hao Zhang, and Ion Stoica. 2023. Efficient Memory Management for Large Language Model Serving with PagedAttention. In *Proceedings of the 29th Symposium on Operating Systems Principles (SOSP)*. 611–626. <https://doi.org/10.1145/3600006.3613165>
- 1423 [45] Chris Lattner, Mehdi Amini, Uday Bondhugula, Albert Cohen, Andy Davis, Jacques Pienaar, River Riddle, Tatiana Shpeisman, Nicolas Vasilache, and Oleksandr Zinenko. 2021. MLIR: Scaling Compiler Infrastructure for Domain Specific Computation. In *Proceedings of the IEEE/ACM International Symposium on Code Generation and Optimization (CGO)*. 2–14. <https://doi.org/10.1109/CGO51591.2021.9370308> Multi-level IR infrastructure enabling cost model composition across abstraction levels.
- 1424 [46] Hyojung Lee, Daehyeon Baek, Jimyoung Son, Jieun Choi, Kihyo Moon, and Minsung Jang. 2025. PAISE: PIM-Accelerated Inference Scheduling Engine for Transformer-based LLM. In *Proceedings of the IEEE International Symposium on High Performance Computer Architecture (HPCA)*. 1–14. PIM-based LLM inference scheduling. 48.3% speedup, 11.5% power reduction. Samsung..
- 1425 [47] Hayeon Lee, Sewoong Lee, Song Chong, and Sung Ju Hwang. 2021. HELP: Hardware-Adaptive Efficient Latency Prediction for NAS via Meta-Learning. In *Advances in Neural Information Processing Systems (NeurIPS)*, Vol. 34. 27016–27028.
- 1426 [48] Seunghyun Lee, Amar Phanishayee, and Divya Mahajan. 2025. NeuSight: GPU Performance Forecasting via Tile-Based Execution Analysis. In *Proceedings of the 30th ACM International Conference on Architectural Support for Programming Languages and Operating Systems (ASPLOS)*. 1–15.

- 1509 [49] Jianbo Li et al. 2025. TrioSim: A Lightweight Simulator for Large-Scale DNN
1510 Workloads on Multi-GPU Systems. In *Proceedings of the 52nd Annual International
1511 Symposium on Computer Architecture (ISCA)*. 1–13. Multi-GPU DNN simulation
1512 with lightweight approach for distributed training analysis.
- 1513 [50] Shang Li, Zhiyuan Yang, Dhiraj Reddy, Ankur Srivastava, and Bruce Jacob. 2020.
1514 DRAMsim3: A Cycle-Accurate, Thermal-Capable DRAM Simulator. *IEEE Computer
1515 Architecture Letters* 19, 2 (2020), 106–109. [https://doi.org/10.1109/LCA.
1516 2020.2973991](https://doi.org/10.1109/LCA.2020.2973991) Modernized DRAM simulator with thermal modeling and HMC
1517 support.
- 1518 [51] Ying Li, Yifan Sun, and Adwait Jogi. 2023. Path Forward Beyond Simulators: Fast
1519 and Accurate GPU Execution Time Prediction for DNN Workloads. In *Proceedings
1520 of the 56th Annual IEEE/ACM International Symposium on Microarchitecture (MICRO)*,
1521 1–14. <https://doi.org/10.1145/3613424.3614277> Linear-regression-based
1522 DNN execution time predictor achieving 7% error for new DNN prediction and 15.2% for new GPU prediction.
- 1523 [52] Wenzuan Liang et al. 2025. Lumos: Efficient Performance Modeling and Estimation
1524 for Large-scale LLM Training. In *Proceedings of Machine Learning and Systems (MLSys)*,
1525 1–16. Trace-driven performance modeling achieving 3.3% error on H100 GPUs for LLM training.
- 1526 [53] Haocong Luo, Yahya Can Tugrul, F. Nisa Bostancı, Ataberk Olgun, A. Giray
1527 Yalçınk, and Onur Mutlu. 2023. Ramulator 2.0: A Modern, Modular, and Extensible
1528 DRAM Simulator. *IEEE Computer Architecture Letters* 22, 2 (2023), 129–132.
1529 <https://doi.org/10.1109/LCA.2023.3333759> Modular DRAM simulator with DDR5,
1530 LPDDR5, HBM3, GDDR6 support and RowHammer mitigation modeling.
- 1531 [54] Peter Mattson, Christine Cheng, Cody Coleman, Greg Diamos, Paulius Micikevicius,
1532 David Patterson, Hanlin Tang, Gu-Yeon Wei, Peter Bailis, Victor Bittorf, et al. 2020.
1533 MLPerf Training Benchmark. In *Proceedings of Machine Learning and Systems (MLSys)*,
1534 336–349. Standard ML training benchmark suite covering image classification, object
1535 detection, NLP, recommendation, reinforcement learning.
- 1536 [55] Azaz-Ur-Rehman Nasir, Samroz Ahmad Shoib, Muhammad Abdullah Hanif, and
1537 Muhammad Shafique. 2025. ESM: A Framework for Building Effective Surrogate
1538 Models for Hardware-Aware Neural Architecture Search. In *Proceedings of the
1539 62nd ACM/IEEE Design Automation Conference (DAC)*. 1–6. 97.6% accuracy
1540 surrogate model framework for HW-aware NAS.
- 1541 [56] Amir Nasr-Esfahany et al. 2025. Concorde: Fast and Accurate CPU Performance
1542 Modeling with Compositional Analytical-ML Fusion. In *Proceedings of the 52nd
1543 Annual International Symposium on Computer Architecture (ISCA)*. 1–15. Hybrid
1544 analytical-ML approach achieving 2% CPI error at 5 orders of magnitude faster
1545 than gem5.
- 1546 [57] NVIDIA Corporation. 2019. Nsight Compute: Interactive Kernel Profiler. <https://developer.nvidia.com/nsight-compute>. Industry-standard GPU kernel profiling
1547 tool with roofline analysis.
- 1548 [58] Angshuman Parashar, Priyanka Raina, Yakun Sophia Shao, Yu-Hsin Chen,
1549 Victor A. Ying, Anurag Muber, Rangharajan Venkatesan, Brucek Khailany,
1550 Stephen W. Keckler, and Joel Emer. 2019. Timeloop: A Systematic Approach
1551 to DNN Accelerator Evaluation. In *Proceedings of the IEEE International Symposium
1552 on Performance Analysis of Systems and Software (ISPASS)*. 304–315.
1553 <https://doi.org/10.1109/ISPASS.2019.00042>
- 1554 [59] Jaehyun Park, Jaewan Choi, Kwanhee Kyung, Michael Jaemini Kim, Yongsuk
1555 Kwon, Nam Sung Kim, and Jung Ho Ahn. 2024. AttAcc! Unleashing the Power of
1556 PIM for Batched Transformer-based Generative Model Inference. In *Proceedings of
1557 the 29th ACM International Conference on Architectural Support for Programming
1558 Languages and Operating Systems (ASPLOS)*. 1–16. PIM-based accelerator for
1559 batched transformer attention. Seoul National University/UIUC..
- 1560 [60] Adam Paszke, Sam Gross, Francisco Massa, Adam Lerer, James Bradbury, Gregory
1561 Chanan, Trevor Killeen, Zeming Lin, Natalia Gimelshein, Luca Antiga, et al. 2019.
1562 PyTorch: An Imperative Style, High-Performance Deep Learning Library. In
1563 *Advances in Neural Information Processing Systems (NeurIPS)*, Vol. 32. 8024–8035.
- 1564 [61] Pratyush Patel, Esha Choukse, Chaojie Zhang, Aakanksha Shah, Íñigo Goiri,
1565 Saeed Maleki, and Ricardo Bianchini. 2024. Splitwise: Efficient Generative LLM
1566 Inference Using Phase Splitting. In *Proceedings of the 51st Annual International
1567 Symposium on Computer Architecture (ISCA)*. 118–132. <https://doi.org/10.1109/ISCA59077.2024.00019> Best Paper Award.
- 1568 [62] Hang Qi, Evan R. Sparks, and Ameet Talwalkar. 2017. Paleo: A Performance
1569 Model for Deep Neural Networks. In *Proceedings of the 5th International Conference
1570 on Learning Representations (ICLR)*. <https://openreview.net/forum?id=SyVvJ85lg>
- 1571 [63] Aurick Qiao, Sang Keun Agrawal, Anand Jayaraman, Moustafa Mittal, Amar Altaf,
1572 Michael Cho, and Gennady Pekhimenko. 2021. Pollux: Co-adaptive Cluster
1573 Scheduling for Goodput-Optimized Deep Learning. In *Proceedings of the 15th
1574 USENIX Symposium on Operating Systems Design and Implementation (OSDI)*,
1575 1–18. Goodput estimation for co-optimizing resource allocation and training
1576 hyperparameters.
- 1577 [64] Jonathan Ragan-Kelley, Connell Barnes, Andrew Adams, Sylvain Paris, Frédo
1578 Durand, and Saman Amarasinghe. 2013. Halide: A Language and Compiler
1579 for Optimizing Parallelism, Locality, and Recomputation in Image Processing
1580 Pipelines. In *Proceedings of the 34th ACM SIGPLAN Conference on Programming
1581 Language Design and Implementation (PLDI)*. 519–530. [https://doi.org/10.1145/
1582 2491956.2462176](https://doi.org/10.1145/2491956.2462176) Pioneered separation of algorithm and schedule with learned
1583 cost models for autoscheduling.
- 1584 [65] Samyam Rajbhandari, Jeff Rasley, Olatunji Rber, and Yuxiong He. 2020. ZERO:
1585 Memory Optimizations Toward Training Trillion Parameter Models. In *Proceedings
1586 of the International Conference on High Performance Computing, Networking,
1587 Storage and Analysis (SC)*. 1–16. <https://doi.org/10.1109/SC41405.2020.00024>
1588 DeepSpeed ZERO optimizer partitioning for memory-efficient distributed training.
- 1589 [66] Mehdi Rakhsanfar and Aliakbar Zarandi. 2021. A Survey on Machine Learning-
1590 based Design Space Exploration for Processor Architectures. *Journal of Systems
1591 Architecture* 121 (2021), 102339. <https://doi.org/10.1016/j.sysarc.2021.102339>
- 1592 [67] Saeed Rashidi, Srinivas Srinivasan, Kazem Hamedani, and Tushar Krishna. 2020.
1593 ASTRA-SIM: Enabling SW/HW Co-Design Exploration for Distributed
1594 DL Training Platforms. In *Proceedings of the IEEE International Symposium
1595 on Performance Analysis of Systems and Software (ISPASS)*. 81–92. <https://doi.org/10.1109/ISPASS48437.2020.00018>
- 1596 [68] Vijay Janapa Reddi et al. 2025. MLPerf Power: Benchmarking the Energy Efficiency
1597 of Machine Learning Inference. In *Proceedings of the IEEE International Symposium
1598 on High Performance Computer Architecture (HPCA)*. 1–14. Energy efficiency
1599 benchmarking for ML inference workloads.
- 1600 [69] Vijay Janapa Reddi, Christine Cheng, David Kanter, Peter Mattson, Guenther
1601 Schmuelling, Carole-Jean Wu, Brian Anderson, Maxim Breeshekov, Mark Duber,
1602 et al. 2020. MLPerf Inference Benchmark. In *Proceedings of the 47th International
1603 Symposium on Computer Architecture (ISCA)*. 446–459. <https://doi.org/10.1109/ISCA45697.2020.00045> Standard ML inference benchmark suite with server and
1604 offline scenarios.
- 1605 [70] George F. Riley and Thomas R. Henderson. 2010. The ns-3 Network Simulator.
1606 *Modeling and Tools for Network Simulation* (2010), 15–34. https://doi.org/10.1007/978-3-642-12331-3_2
- 1607 [71] Arun F. Rodrigues, K. Scott Hemmert, Brian W. Barrett, Chad Kersey, Ron Oldfield,
1608 Marlo Weston, R. Risen, Jeanine Cook, Paul Rosenfeld, Elliott Cooper-Balis, and
1609 Bruce Jacob. 2012. The Structural Simulation Toolkit. In *ACM SIGMETRICS Performance
1610 Evaluation Review*, Vol. 38. 37–42. <https://doi.org/10.1145/1964218.1964225> Modular framework for system-level simulation, widely used for HPC
1611 and interconnect modeling.
- 1612 [72] Ananda Samajdar, Yuhao Zhu, Paul Whatmough, Matthew Mattina, and Tushar
1613 Krishna. 2019. A Systematic Methodology for Characterizing Scalability of
1614 DNN Accelerators using SCALE-Sim. In *Proceedings of the IEEE International
1615 Symposium on Performance Analysis of Systems and Software (ISPASS)*. 58–68.
1616 <https://doi.org/10.1109/ISPASS.2019.00016> Cycle-accurate systolic array simulator
1617 for DNN accelerator DSE.
- 1618 [73] Zhuomin Shen, Jaeho Kim, et al. 2025. AQUA: Network-Accelerated Memory
1619 Offloading for LLMs in Scale-Up GPU Domains. In *Proceedings of the 30th ACM
1620 International Conference on Architectural Support for Programming Languages
1621 and Operating Systems (ASPLOS)*. 1–16. <https://doi.org/10.1145/3676641.3715983>
1622 Improves LLM inference responsiveness by 20x through network-accelerated
1623 memory offloading.
- 1624 [74] Mohammad Shoeybi, Mostofa Patwary, Raul Puri, Patrick LeGresley, Jared Casper,
1625 and Bryan Catanzaro. 2020. Megatron-LM: Training Multi-Billion Parameter
1626 Language Models Using Model Parallelism. In *arXiv preprint arXiv:1909.08053*.
1627 Intra-layer tensor parallelism for large language model training.
- 1628 [75] Srinivas Sridharan, Taekyung Heo, Jinwoo Choi, Garyfallia Yu, Saeed Rashidi,
1629 William Won, Zhaodong Meng, and Tushar Krishna. 2023. Chakra: Advancing
1630 Performance Benchmarking and Co-design using Standardized Execution Traces.
1631 *arXiv preprint arXiv:2305.14516* (2023).
- 1632 [76] Foteini Strati, Zhendong Zhang, George Manos, Ixeia Sanchez Periz, Qinghao
1633 Hu, Tiancheng Chen, Berk Buzcu, Song Han, Pamela Delgado, and Ana Klimovic.
1634 2025. Sailor: Automating Distributed Training over Dynamic, Heterogeneous,
1635 and Geo-distributed Clusters. In *Proceedings of the 30th ACM Symposium on
1636 Operating Systems Principles (SOSP)*. 1–18. Automated distributed training with
1637 runtime/memory simulation over heterogeneous resources. ETH Zurich/MIT..
- 1638 [77] Jonas Svedas, Hannah Watson, Nathan Laubeuf, Diksha Moolchandani, Abubakr
1639 Nada, Arjun Singh, Dwaipayan Biswas, James Myers, and Debjyoti Bhattacharjee.
1640 2025. A Survey of End-to-End Modeling for Distributed DNN Training: Workloads,
1641 Simulators, and TCO. *arXiv preprint arXiv:2506.09275* (2025). Comprehensive survey of distributed DNN training simulators covering workload
1642 representation, simulation infrastructure, and TCO/carbon modeling.
- 1643 [78] Ondrej Sykora, Alexis Rucker, Charith Mendis, Rajkishore Barik,
1644 Phitchaya Mangpo Phothilimhana, and Saman Amarasinghe. 2022. GRANITE:
1645 A Graph Neural Network Model for Basic Block Throughput Estimation. In
1646 *Proceedings of the IEEE International Symposium on Workload Characterization
1647 (IISWC)*. 1–13. <https://doi.org/10.1109/IISWC55918.2022.00014>
- 1648 [79] Vivienne Sze, Yu-Hsin Chen, Tien-Ju Yang, and Joel S. Emer. 2017. Efficient
1649 Processing of Deep Neural Networks: A Tutorial and Survey. In *Proceedings
1650 of the IEEE*, Vol. 105. 2295–2329. <https://doi.org/10.1109/JPROC.2017.2761740> Canonical DNN accelerator taxonomy covering dataflows, data reuse, and energy
1651

- 1625 efficiency.
- 1626 [80] Philippe Tillet, H. T. Kung, and David Cox. 2019. Triton: An Intermediate Lan-
1627 guage and Compiler for Tiled Neural Network Computations. In *Proceedings
1628 of the 3rd ACM SIGPLAN International Workshop on Machine Learning and Pro-
1629 gramming Languages (MAPL)*. 10–19. <https://doi.org/10.1145/3315508.3329973>
- 1630 Tile-based GPU programming with heuristic performance model for kernel
1631 generation.
- 1632 [81] Jan Treibig, Georg Hager, and Gerhard Wellein. 2010. LIKWID: A Lightweight
1633 Performance-Oriented Tool Suite for x86 Multicore Environments. In *Proceedings
1634 of the 39th International Conference on Parallel Processing Workshops (ICPPW)*. 207–
1635 216. <https://doi.org/10.1109/ICPPW.2010.38> Lightweight tools for thread/cache
1636 topology, affinity, and performance counter measurement.
- 1637 [82] Adrian Tschanz, Mohamed Awad, et al. 2025. SwizzlePerf: Hardware-Aware
1638 LLMs for GPU Kernel Performance Optimization. *arXiv preprint arXiv:2508.20258*
1639 (2025). LLM-based spatial optimization for GPU kernels, up to 2.06x speedup
1640 via swizzling.
- 1641 [83] Xizheng Wang, Qingxu Li, Yichi Xu, Gang Lu, Heyang Zhou, Sen Zhang, Yikai
1642 Zhu, Yang Liu, Pengcheng Zhang, Kun Qian, et al. 2025. SimAI: Unifying Ar-
1643 chitecture Design and Performance Tuning for Large-Scale LLM Training with
1644 Scalability and Precision. In *Proceedings of the 22nd USENIX Symposium on
1645 Networked Systems Design and Implementation (NSDI)*. 1–18. Full-stack LLM
1646 training simulator achieving 98.1% alignment with real-world results. Alibaba
1647 Cloud/Tsinghua..
- 1648 [84] Zixian Wang et al. 2025. SynPerf: Synthesizing High-Performance GPU Kernels
1649 via Pipeline Decomposition. *arXiv preprint* (2025). Under review.
- 1650 [85] Samuel Williams, Andrew Waterman, and David Patterson. 2009. Roofline: An
1651 Insightful Visual Performance Model for Multicore Architectures. *Commun.
1652 ACM* 52, 4 (2009), 65–76. <https://doi.org/10.1145/1498765.1498785>
- 1653 [86] William Won, Taekyung Heo, Saeed Rashidi, Saeed Talati, Srinivas Srinivasan,
1654 and Tushar Krishna. 2023. ASTRA-sim2.0: Modeling Hierarchical Networks and
1655 Disaggregated Systems for Large-Model Training at Scale. In *Proceedings of the
1656 IEEE International Symposium on Performance Analysis of Systems and Software
1657 (ISPASS)*. 283–294. <https://doi.org/10.1109/ISPASS57527.2023.00035>
- 1658 [87] Yannan Nellie Wu, Joel Emer, and Vivienne Sze. 2022. Sparseloop: An Analytical
1659 Approach to Sparse Tensor Accelerator Modeling. In *Proceedings of the 55th
1660 International Symposium on Microarchitecture (MICRO)*. 1–15. <https://doi.org/10.1109/MICRO56248.2022.000078>
- 1661 [88] Gyeong-In Yu, Joo Seong Jeong, Geon-Woo Kim, Soojeong Kim, and Byung-
1662 Gon Chun. 2022. ORCA: A Distributed Serving System for Transformer-Based
1663 Generative Models. In *Proceedings of the 16th USENIX Symposium on Operating
1664 Systems Design and Implementation (OSDI)*. 521–538.
- 1665 [89] Geoffrey X. Yu, Yubo Gao, Pavel Golber, and Asaf Cidon. 2021. Habitat: A
1666 Runtime-Based Computational Performance Predictor for Deep Neural Network
1667 Training. In *Proceedings of the USENIX Annual Technical Conference (ATC)*. 503–
1668 521.
- 1669 [90] Yi Zhai, Yu Cheng Wang, Peng Jiang, and Congming Kang. 2023. TLP: A Deep
1670 Learning-based Cost Model for Tensor Program Tuning. In *Proceedings of the
1671 28th ACM International Conference on Architectural Support for Programming
1672 Languages and Operating Systems (ASPLOS)*. 833–845. <https://doi.org/10.1145/3575693.3575736>
- 1673 [91] Li Lyra Zhang, Shihao Han, Jianyu Wei, Ningxin Zheng, Ting Cao, Yuqing Yang,
1674 and Yunxin Liu. 2021. nn-Meter: Towards Accurate Latency Prediction of Deep-
1675 Learning Model Inference on Diverse Edge Devices. In *Proceedings of the 19th
1676 Annual International Conference on Mobile Systems, Applications, and Services
1677 (MobiSys)*. 81–93. <https://doi.org/10.1145/3458864.3467882> Best Paper Award.
- 1678 [92] Lianmin Zheng, Chengfan Jia, Minmin Sun, Zhao Wu, Cody Hao Yu, Ameer
1679 Haj-Ali, Yida Wang, Jun Yang, Danyang Zhuo, Koushik Sen, Joseph E. Gonzalez,
1680 and Ion Stoica. 2020. AnsoR: Generating High-Performance Tensor Programs
1681 for Deep Learning. In *Proceedings of the 14th USENIX Symposium on Operating
1682 Systems Design and Implementation (OSDI)*. 863–879.
- 1683 [93] Lianmin Zheng, Ruochen Liu, Junru Shao, Tianqi Chen, Joseph E. Gonzalez,
1684 Ion Stoica, and Zhihao Zhang. 2021. TenSet: A Large-scale Program Perfor-
1685 mance Dataset for Learned Tensor Compilers. In *Advances in Neural Information
1686 Processing Systems (NeurIPS)*, Vol. 34. 29876–29888.
- 1687 [94] Yinmin Zhong, Shengyu Liu, Junda Chen, Jianyu Hu, Yibo Zhu, Xuanzhe Liu,
1688 Xin Jin, and Hao Zhang. 2024. DistServe: Disaggregating Prefill and Decoding
1689 for Goodput-optimized Large Language Model Serving. In *Proceedings of the 18th
1690 USENIX Symposium on Operating Systems Design and Implementation (OSDI)*.
1691 1–18.
- 1692 [95] Lianmin Zheng, Ruochen Liu, Junru Shao, Tianqi Chen, Joseph E. Gonzalez,
1693 Ion Stoica, and Zhihao Zhang. 2021. TenSet: A Large-scale Program Perfor-
1694 mance Dataset for Learned Tensor Compilers. In *Advances in Neural Information
1695 Processing Systems (NeurIPS)*, Vol. 34. 29876–29888.
- 1696 [96] Lianmin Zheng, Ruochen Liu, Junru Shao, Tianqi Chen, Joseph E. Gonzalez,
1697 Ion Stoica, and Zhihao Zhang. 2021. TenSet: A Large-scale Program Perfor-
1698 mance Dataset for Learned Tensor Compilers. In *Advances in Neural Information
1699 Processing Systems (NeurIPS)*, Vol. 34. 29876–29888.
- 1700 [97] Lianmin Zheng, Ruochen Liu, Junru Shao, Tianqi Chen, Joseph E. Gonzalez,
1701 Ion Stoica, and Zhihao Zhang. 2021. TenSet: A Large-scale Program Perfor-
1702 mance Dataset for Learned Tensor Compilers. In *Advances in Neural Information
1703 Processing Systems (NeurIPS)*, Vol. 34. 29876–29888.
- 1704 [98] Yinmin Zhong, Shengyu Liu, Junda Chen, Jianyu Hu, Yibo Zhu, Xuanzhe Liu,
1705 Xin Jin, and Hao Zhang. 2024. DistServe: Disaggregating Prefill and Decoding
1706 for Goodput-optimized Large Language Model Serving. In *Proceedings of the 18th
1707 USENIX Symposium on Operating Systems Design and Implementation (OSDI)*.
1708 1–18.
- 1709 [99] Lianmin Zheng, Ruochen Liu, Junru Shao, Tianqi Chen, Joseph E. Gonzalez,
1710 Ion Stoica, and Zhihao Zhang. 2021. TenSet: A Large-scale Program Perfor-
1711 mance Dataset for Learned Tensor Compilers. In *Advances in Neural Information
1712 Processing Systems (NeurIPS)*, Vol. 34. 29876–29888.
- 1713 [100] Lianmin Zheng, Ruochen Liu, Junru Shao, Tianqi Chen, Joseph E. Gonzalez,
1714 Ion Stoica, and Zhihao Zhang. 2021. TenSet: A Large-scale Program Perfor-
1715 mance Dataset for Learned Tensor Compilers. In *Advances in Neural Information
1716 Processing Systems (NeurIPS)*, Vol. 34. 29876–29888.
- 1717 [101] Lianmin Zheng, Ruochen Liu, Junru Shao, Tianqi Chen, Joseph E. Gonzalez,
1718 Ion Stoica, and Zhihao Zhang. 2021. TenSet: A Large-scale Program Perfor-
1719 mance Dataset for Learned Tensor Compilers. In *Advances in Neural Information
1720 Processing Systems (NeurIPS)*, Vol. 34. 29876–29888.
- 1721 [102] Lianmin Zheng, Ruochen Liu, Junru Shao, Tianqi Chen, Joseph E. Gonzalez,
1722 Ion Stoica, and Zhihao Zhang. 2021. TenSet: A Large-scale Program Perfor-
1723 mance Dataset for Learned Tensor Compilers. In *Advances in Neural Information
1724 Processing Systems (NeurIPS)*, Vol. 34. 29876–29888.
- 1725 [103] Lianmin Zheng, Ruochen Liu, Junru Shao, Tianqi Chen, Joseph E. Gonzalez,
1726 Ion Stoica, and Zhihao Zhang. 2021. TenSet: A Large-scale Program Perfor-
1727 mance Dataset for Learned Tensor Compilers. In *Advances in Neural Information
1728 Processing Systems (NeurIPS)*, Vol. 34. 29876–29888.
- 1729 [104] Lianmin Zheng, Ruochen Liu, Junru Shao, Tianqi Chen, Joseph E. Gonzalez,
1730 Ion Stoica, and Zhihao Zhang. 2021. TenSet: A Large-scale Program Perfor-
1731 mance Dataset for Learned Tensor Compilers. In *Advances in Neural Information
1732 Processing Systems (NeurIPS)*, Vol. 34. 29876–29888.
- 1733 [105] Lianmin Zheng, Ruochen Liu, Junru Shao, Tianqi Chen, Joseph E. Gonzalez,
1734 Ion Stoica, and Zhihao Zhang. 2021. TenSet: A Large-scale Program Perfor-
1735 mance Dataset for Learned Tensor Compilers. In *Advances in Neural Information
1736 Processing Systems (NeurIPS)*, Vol. 34. 29876–29888.
- 1737 [106] Lianmin Zheng, Ruochen Liu, Junru Shao, Tianqi Chen, Joseph E. Gonzalez,
1738 Ion Stoica, and Zhihao Zhang. 2021. TenSet: A Large-scale Program Perfor-
1739 mance Dataset for Learned Tensor Compilers. In *Advances in Neural Information
1740 Processing Systems (NeurIPS)*, Vol. 34. 29876–29888.